

To

Prof. Veli-Matti Kerminen  
Editor  
Atmospheric Chemistry and Physics (ACP)

**RE:** Submission of revised manuscript entitled:

**“Dicarboxylic acids, oxoacids, benzoic acid,  $\alpha$ -dicarbonyls, WSOC, OC, and ions in spring aerosols from Okinawa Island in the western North Pacific Rim: Size distributions and formation processes”**

for publication in Atmospheric Chemistry and Physics

**Reference:** MS No.: acp-2015-568

Dear Prof. Kerminen,

Thanks for the decision letter on our paper. The authors greatly appreciate the useful comments by anonymous referees to improve the scientific content of our paper. We responded to all the queries in the revised MS. Our responses and changes are briefly described in the response letter as blue color. The changes in the revision are highlighted in yellow.

We believe that the revised MS can be acceptable for publication in ACP.

Thanking you.

Sincerely yours,

Kimitaka Kawamura  
Professor of Chemistry  
Institute of Low Temperature Science  
Hokkaido University  
Sapporo 060-0819  
Japan  
E-mail: kawamura@lowtem.hokudai.ac.jp  
kkawamura@isc.chubu.ac.jp

## **Responses to the Comments of Referee #2**

The revised manuscript was evaluated. The discussion for the inorganic ions has been improved considerably. However, it was still hard to follow the discussion for the organic components. As proven by the 27 “may”s in the text, the revised manuscript still had too many speculations to explain the observations during this case study. Particularly, it was hard to follow the discussion on the oxidative production of organic components in aqueous droplets. There were also some points that the authors did not seem to address in the revision (e.g., line 354-357). I still saw many writing issues too, such as tense (i.e., mixing present and past tense as referring the observed results), conciseness (e.g., line 434-438), etc. After reading it, I am impressed unfortunately that the revised manuscript is still not an acceptable form by ACP.

**Response:** We thank the referee’s critical reading and useful comments that helped us to make our manuscript concise (shortened by 4 pages) and improve the scientific content of the paper. The manuscript has been rigorously checked for its correctness towards interpretation and discussion of the data observed.

We found strong positive correlations of oxidation products with LWC in fine mode, indicating a possible production of water-soluble organic compounds (and  $\text{SO}_4^{2-}$ ) in aqueous-phase. Following the referee’s comments, the discussion on the formation of fine mode  $\text{SO}_4^{2-}$  in cloud droplets has been deleted and appropriate changes have been made in the revised MS. The discussion on the results of correlation analysis between LWC and major inorganic ions ( $\text{SO}_4^{2-}$  and  $\text{NH}_4^+$ ) has now been deleted. The revised MS has been edited for the English language.

Please see our responses below and the revised MS.

The followings are specific points I would like to make.

Specific comments:

Figure 2 is still confusing. The authors should provide the time information (in UTC or local time) for the trajectories as well.

**Response:** To avoid any confusion, we have given the typical air mass trajectories corresponding to 0900 UTC for the samples collected in Okinawa. Please see Figure S1 in the supporting information and lines 155-156 in the revised MS.

As per the suggestion of referee #3, we have provided vertical profile of air mass trajectories in Figure 2 in the revised MS.

In the text the discussion the authors are making with Figure 3 is about the overall chemical composition in the “fine” and “coarse” modes of particles. Such information is available from Table 1. I still do not see a point that the authors need to show Figure 3. This point has not been improved.

**Response:** Following the referee’s comment, we have deleted Figure 3 in the revised MS.

Line 186: The reference by Takiguchi et al. does not seem to show the analytical results of organic aerosols, but nitrate aerosols. This group has published a better publication showing the analysis of oxygenated organic aerosols in Okinawa (Irei et al., EST, 2014). This reference seems more appropriate in this case.

**Response:** Following the referee’s suggestion, we have replaced “Takiguchi et al. 2008” by “Irei et al. 2014”. Please see lines 183 and 661-664 in the revised MS.

Line 215-223: A writing issue. The authors should be able to organize the possible sources of C2 more concisely.

**Response:** We have reorganized the sentence as follows.

“The predominance of  $C_2$  in size-segregated aerosols is due to the fact that it can be secondarily produced by the photooxidation of anthropogenic and biogenic organic precursors in gas and aqueous-phase (Kawamura and Sakaguchi, 1999; Warneck, 2003; Carlton et al., 2006).  $C_2$  can also be produced primarily from fossil fuel combustion (Kawamura and Kaplan, 1987) and biomass burning (Kundu et al., 2010) in East Asia and long-range transported to Okinawa.”

Please see lines 212-217 in the revised MS.

Line 300-302: State explicitly that the particle size grew during the long-range transport.

**Response:** We have revised the sentence as below.

“The peak of  $K^+$  at 0.65-1.1  $\mu\text{m}$  suggests that biomass burning particles emitted in East Asia might have undergone a growth to a relatively large size by absorbing water vapor from the atmosphere during long-range transport to Okinawa.”

Please see lines 290-292 in the revised MS.

Line 341-347 and line 464-475: To explain the observed results of oxidation products found in the fine mode, the authors hypothesized that photooxidation occurred first in cloud droplets, which must be in large size, and then the droplets dried and shrank to smaller size. Did the authors find any supporting result for this particle shrink from the model calculation of LWC? If the latter assumption really happened, I expect that the oxidation products and the LWC were anti-correlated because the particles were dried. Contradictorily, the authors state later that the high correlation was observed between the ratio of WSOC, a group of oxidation products, to OC (or  $\text{SO}_4^{2-}$ , for example) and LWC. The logic does not make sense...It will be worthwhile to show time series plot of temperature, RH, and the calculated LWC during the sampling periods (from March 18 to April 13) so that the hypothesis of particle shrink is partially supported by own data.

**Response:** We agree with the referee's comment that oxidation products and LWC were anti-correlated if shrinking of cloud droplets happened in our samples. However, we found strong positive correlations of oxidation products with LWC in fine mode (Table 2), indicating a possible production of water-soluble organic compounds (and  $\text{SO}_4^{2-}$ ) in aqueous-phase. Therefore, we are not going to conclude the formation of fine mode  $\text{SO}_4^{2-}$  in cloud droplets in the revised MS. However, fine mode  $\text{SO}_4^{2-}$  ( $D_p$  0.65-1.1  $\mu\text{m}$ ) can be formed via oxidation of  $\text{SO}_2$  in aerosol aqueous-phase. Therefore, we have revised the text as follows.

“A unimodal size distribution of  $\text{SO}_4^{2-}$  was observed with a peak at 0.65-1.1  $\mu\text{m}$  (Figure 4g). Gao et al. (2012) suggested that in-cloud process produces  $\text{SO}_4^{2-}$  as larger particles by aqueous-phase oxidation of  $\text{SO}_2$  in cloud droplets. Therefore, the peak of  $\text{SO}_4^{2-}$  at 0.65-1.1  $\mu\text{m}$  in Okinawa may be involved with aqueous-phase oxidation of  $\text{SO}_2$  in aerosols.”

Please see lines 325-329 in the revised MS.

Line 428-431: I cannot follow the logic why the high loading of WSOC suggests significant contribution from fossil fuel combustion and biomass burning.

**Response:** Following the referee's comment, we have removed the phrase: “Because WSOC is an.....North Pacific Rim” in the revised MS.

Line 646-654: I cannot follow the logic. The authors ruled out a possibility that the observed  $wC_9$  originated from sea-surface microlayer. Does the microlayer never contain  $wC_9$ ? The authors should show scientific evidence using references or observations.

**Response:** We have revised the text as follows.

“The strong correlations were found between  $C_9$  and  $\text{Na}^+$  ( $r = 0.85$ ), and  $\omega C_9$  and  $\text{Na}^+$  (0.83) in

coarse mode, indicating that  $C_9$  and  $\omega C_9$  may be emitted into the atmosphere from the sea surface microlayers together with sea salt particles in Okinawa. Kawamura and Gagosian (1987) suggested that  $C_9$  and  $\omega C_9$  are also derived from the photooxidation of unsaturated fatty acids such as oleic acid ( $C_{18:1}$ ) that are produced by phytoplankton and emitted from sea surface microlayers as sea salt particles. The laboratory experiments also documented the formation of  $C_9$  and  $\omega C_9$  due to photooxidation of  $C_{18:1}$  (Matsunaga et al., 1999; Huang et al., 2005; Ziemann, 2005; Tedetti et al., 2007). Sea surface microlayers in the surroundings of Okinawa can also emit unsaturated fatty acids together with sea salts. Therefore, the major peaks of  $C_9$  and  $\omega C_9$  on the coarse mode may be derived from heterogeneous oxidation of unsaturated fatty acids of marine phytoplankton origin on the sea salt particles.”

Please see lines 543-553 in the revised MS.

Scatter plot of oxalic acid concentration vs. other organic compound concentration:  $N=5$  does not sound an acceptable reason for excluding this plot from the paper because the authors are submitting this manuscript based on the 5 sample analysis anyway. Correlation coefficients for some linear regressions seem to be very high, indicating something. Error analysis should be used to judge that the slopes themselves and the differences between the slopes are significant. The authors should scientifically analyze the plots a little more deeply.

**Response:** We have given scatter plots of oxalic acid ( $C_2$ ) with its next higher diacids ( $C_3$ - $C_5$ ), glyoxylic acid ( $\omega C_2$ ) and glyoxal (Gly) in Figure S3. Correlation coefficients and slopes of the regression lines between  $C_2$  and other diacids and related compounds are also provided in Table S1 and S2 together with their statistical significance (t-test). The following sentences have been added towards the discussion on the slope of the regression lines of  $C_2$  with other organic compounds.

“The scatter plots of  $C_2$  with  $C_3$ - $C_5$  diacids in fine and coarse modes are shown in Figure S3. The robust correlations of  $C_2$  with  $C_3$ - $C_5$  diacids ( $r = 0.89$ - $0.92$ ) were found in fine mode, indicating that they might have similar sources and origin or  $C_2$  may be produced via the decay of its higher homologues ( $C_3$ - $C_5$  diacids) during long-range transport. The differences in the slopes of linear regression of  $C_2$  with  $C_3$  and  $C_4$  diacids between fine and coarse modes are not significant but slopes are slightly higher in fine mode than the coarse mode (Figure S3a-d and Table S1). Interestingly, significantly higher slope was observed for regression line between  $C_2$  and glutaric ( $C_5$ ) acid in fine mode than coarse mode (Figure S3e-f and Table S1). It is also noteworthy that the slope of regression line of  $C_2$  with  $C_5$  diacid is significantly higher than that for  $C_3$  and  $C_4$  diacids in fine mode (Figure S3a, c, e and Table S2). These results indicate that fine mode oxalic acid may be produced from oxidation of glutaric acid during long-range transport via succinic and malonic acids as intermediates. The laboratory studies of Hatakeyama et al. (1985) and Kalberer et al. (2010) have documented that glutaric acid is produced by the oxidation of cyclohexene by  $O_3$ , which can be further oxidized in aqueous-phase to result in oxalic acid (Kawamura and Sakaguchi, 1999; Legrand et al., 2007).”

“There is no significant difference in the slope of regression line of  $C_2$  with  $\omega C_2$  between the fine and coarse modes (Figure S3g-h and Table S1) whereas the slope of regression line of  $C_2$  with Gly is significantly higher in fine mode than coarse mode (Figure S3i-j and Table S1). It is also remarkable that the slope of linear regression of  $C_2$  with Gly is significantly higher than that with  $\omega C_2$  in fine mode (Figure S3g-i and Table S2). This result may indicate a possible formation of fine mode oxalic acid from glyoxal via glyoxylic acid as an intermediate during long-range atmospheric transport in the western North Pacific.”

Please see Figure S3, Table S1 and Table S2, and lines 477-491 and 508-514 in the revised MS.

### **Responses to the Comments of Referee #3**

Lines 157-164 and 189-198 in the revised manuscript:

While the authors made effort to address my comments, it did not address whether the air masses experienced precipitation events DURING the transport (not at the source or the sampling point). The HYSPLIT model can produce meteorological data such as precipitation data along a trajectory so the authors should be able to include this data and discuss about it in the revised manuscript. In addition to this, the HYSPLIT can generate downward solar radiation flux data so this should also be included in the discussion about photochemical production of WSOC from OC in aerosol aqueous-phase (Lines 464-475 in the revised manuscript).

**Response:** Following the suggestions, we have provided the backward air mass trajectories along with the precipitation and downward solar radiation flux data obtained from the HYSPLIT model as supporting information. The following sentences have been added regarding the effect of precipitation and photochemical production of WSOC from OC in aerosol aqueous-phase in the revised MS.

“Precipitation may have an insignificant effect on the transport of pollutants from the source region to Okinawa because air masses were not experienced serious precipitation events during the transport (Figure S2a).”

“The WSOC/OC ratio in fine mode showed a weak positive correlation with downward solar radiation flux ( $r = 0.39$ ). This weak correlation is probably due to the fact that fine mode WSOC can be produced in aqueous-phase of aerosols during long-range transport. Based on the year round measurements of TSP aerosols from Okinawa Island, Kunwar and Kawamura (2014) documented higher WSOC/OC ratio in winter (ave. 0.60) and spring (ave. 0.45) than summer (ave. 0.28). These observations demonstrate that WSOC can be produced from OC under weak solar radiation condition on the transport pathway from the source region to Okinawa possibly via aqueous-phase processing.”

Please see Figure S2, and lines 194-196 and 417-424 in the revised MS.

In connection to HYSPLIT model results, the vertical profiles of trajectories must be included in the Figure 2. When the vertical profiles show a contact with the ground, subsequent air mass movements are not very accurate.

**Response:** We have provided the vertical profile of air mass trajectories in the revised MS. Please see Figure 2.

Line 383-389 in the revised manuscript:

Shouldn't ISORROPIA II predict the state of  $H^+$ ,  $NH_4^+$ ,  $SO_4^{2-}$ , and  $NO_3^-$  in the particle phase? This needs to be discussed in the revised manuscript as well.

**Response:** ISORROPIA II gives the chemical composition in the solid-phase and liquid-phase. ISORROPIA II model calculation results show that significant amounts of  $SO_4^{2-}$ ,  $HSO_4^-$  and  $NH_4^+$  are present in the liquid-phase in fine mode aerosols in Okinawa. We found fine mode  $SO_4^{2-}$  in solid-phase as  $CaSO_4$  in very small amount whereas fine mode  $NH_4^+$  and  $NO_3^-$  are not present in solid-phase. Moreover, coarse mode  $NO_3^-$  and  $SO_4^{2-}$  are present in solid-phase as  $Ca(NO_3)_2$  and  $CaSO_4$ , respectively. Therefore, we have modified the text with a brief discussion in the revised MS as follows.

“The average  $NH_4^+/SO_4^{2-}$  equivalent ratios in fine mode particles in Okinawa varied from 0.36 for the size bin of 1.1-2.1  $\mu m$  to 0.81 for the size bin of 0.43-0.65  $\mu m$ , indicating that  $NH_3$  was not abundant enough to neutralize all  $SO_2$ . The aerosol chemical composition data obtained from the ISORROPIA II model revealed that significant amounts of  $SO_4^{2-}$ ,  $HSO_4^-$  and  $NH_4^+$  in fine mode were present in liquid-phase whereas  $SO_4^{2-}$  and  $NO_3^-$  were mainly present as solid-phase in the

coarse mode aerosols in the forms of  $\text{CaSO}_4$  and  $\text{Ca}(\text{NO}_3)_2$ , respectively.”  
Please see lines 358-364 in the re-revised MS.

Section 3.4 onwards:

I do not agree with the authors' reasons for keeping the structure of these sections. While the authors present the size distribution data on some of “not so common in the literature” organic acids, they are not that useful to the readers if they are just presented in a report style as the case here. I ask the authors to group them based on the formation mechanisms instead of compound groups because that can make this section much more concise and scientifically interesting. As is now, the section is very descriptive and repetitive. It may be acceptable to present such a report style paper when these compounds were newly discovered but I do not see the readers excited to see yet another paper with lots of organic compounds in tables. I believe this manuscript can be improved if the authors address this issue.

**Response:** Thank you very much for the critical comment that helped us to make our manuscript more concise and improve the scientific content of the paper. To better understand the sources and formation processes of Okinawa aerosols, we have grouped the measured diacids and related compounds into two classes. The first group ( $\text{C}_2$ ,  $\omega\text{C}_2$ , Gly, Ph and benzoic acid) shows maxima in the fine mode with a significant influence of anthropogenic sources whereas the second group ( $\text{C}_9$  and  $\omega\text{C}_9$ ) shows maxima in the coarse mode with an influence of biogenic sources. Because we discussed only most interesting target compounds in the text, the appropriate changes have been made in Figure 5 in the revised MS.

Please see lines 439-558.

Because of changing the structure of Section 3.4 onwards, the ratios of diacids ( $\text{C}_3/\text{C}_4$  and  $\text{Ph}/\text{C}_9$ ) have been moved to new section (Section 3.5) in the revised MS.

Concerning Table 2, the authors prefer to keep it as the present style because it is a summary of our results and not for individual samples. We believe that the summary table should be helpful for the readers to better understand our results.

1 **Dicarboxylic acids, oxoacids, benzoic acid,  $\alpha$ -dicarbonyls, WSOC, OC, and ions in spring**  
2 **aerosols from Okinawa Island in the western North Pacific Rim: Size distributions and**  
3 **formation processes**

4 **D. K. Deshmukh<sup>1,2</sup>, K. Kawamura<sup>1,2\*</sup>, M. Lazaar<sup>1,3</sup>, B. Kunwar<sup>1</sup>, and S. K. R. Boreddy<sup>1</sup>**

5 <sup>1</sup>**Institute of Low Temperature Science, Hokkaido University, Sapporo 060-0819, Japan**

6 <sup>2</sup>**Now at Chubu Institute for Advanced Studies, Chubu University, Kasugai 487-8501, Japan**

7 <sup>3</sup>**Ecole National Supérieure de Chimie de Rennes (ENSCR), Rennes 35708, France**

8 \*Corresponding author

9 E-mail address: [kkawamura@isc.chubu.ac.jp](mailto:kkawamura@isc.chubu.ac.jp)

## 10 Abstract

11 Size-segregated aerosols (9-stages from  $<0.43$  to  $>11.3$   $\mu\text{m}$  in diameter) were collected at Cape  
12 Hedo, Okinawa in spring 2008 and analyzed for water-soluble diacids ( $\text{C}_2\text{-C}_{12}$ ),  $\omega$ -oxoacids ( $\omega\text{C}_2\text{-}$   
13  $\omega\text{C}_9$ ), pyruvic acid, benzoic acid and  $\alpha$ -dicarbonyls ( $\text{C}_2\text{-C}_3$ ) as well as water-soluble organic carbon  
14 (WSOC), organic carbon (OC) and major ions ( $\text{Na}^+$ ,  $\text{NH}_4^+$ ,  $\text{K}^+$ ,  $\text{Mg}^{2+}$ ,  $\text{Ca}^{2+}$ ,  $\text{Cl}^-$ ,  $\text{NO}_3^-$ ,  $\text{SO}_4^{2-}$ , and  
15  $\text{MSA}^-$ ). In all the size-segregated aerosols, oxalic acid ( $\text{C}_2$ ) was found as the most abundant species  
16 followed by malonic and succinic acids whereas glyoxylic acid ( $\omega\text{C}_2$ ) was the dominant oxoacid  
17 and glyoxal (Gly) was more abundant than methylglyoxal. Diacids ( $\text{C}_2\text{-C}_5$ ),  $\omega\text{C}_2$  and Gly as well as  
18 WSOC and OC peaked at fine mode ( $0.65\text{-}1.1$   $\mu\text{m}$ ) whereas azelaic ( $\text{C}_9$ ) and 9-oxononanoic ( $\omega\text{C}_9$ )  
19 acids peaked at coarse mode ( $3.3\text{-}4.7$   $\mu\text{m}$ ). Sulfate and ammonium were enriched in fine mode  
20 whereas sodium and chloride were in coarse mode. Strong correlations of  $\text{C}_2\text{-C}_5$  diacids,  $\omega\text{C}_2$  and  
21 Gly with sulfate were observed in fine mode ( $r = 0.86\text{-}0.99$ ), indicating a commonality in their  
22 secondary formation. Their significant correlations with liquid water content in fine mode ( $r = 0.82\text{-}$   
23  $0.95$ ) further suggest an importance of the aqueous-phase production in Okinawa aerosols. They  
24 may also have been directly emitted from biomass burning in fine mode as supported by strong  
25 correlations with potassium ( $r = 0.85\text{-}0.96$ ), which is a tracer of biomass burning. Bimodal size  
26 distributions of longer-chain diacid ( $\text{C}_9$ ) and oxoacid ( $\omega\text{C}_9$ ) with a major peak in the coarse mode  
27 suggest that they were emitted from the sea surface microlayers and/or produced by heterogeneous  
28 oxidation of biogenic unsaturated fatty acids on sea salt particles.

29 **Keywords:** Water-soluble organic species, ions, size-segregated aerosols, unimodal distribution,  
30 bimodal distribution, secondary aerosols.



## 31 **1 Introduction**

32 Tropospheric aerosol is an important environmental issue because it dramatically reduces the  
33 visibility (Jacobson et al., 2000; Kanakidou et al., 2005), affects the radiative forcing of climate  
34 (Seinfeld and Pandis, 1998), and causes a negative impact on human health (Pope and Dockery,  
35 2006). All of these effects strongly depend on the abundances of aerosols and their chemical and  
36 physical properties in different sizes. Particles in diameter of 0.1-1.0  $\mu\text{m}$  are very active in  
37 scattering and absorbing incoming solar radiation and have a direct impact on climate (Ramanathan  
38 et al., 2001; Seinfeld and Pankow, 2003). The knowledge of size distributions of chemical  
39 components is thus essential to better understand their potential contributions to climate change and  
40 pollution control. Their size distribution also provides evidences for the sources and formation  
41 pathways of atmospheric particles.

42 The emission sources and multiple secondary formation pathways of organic aerosols are not  
43 well understood. Organic compounds account for up to 70% of fine aerosol mass and potentially  
44 control the physicochemical properties of aerosol particles (Davidson et al., 2005; Kanakidou et al.,  
45 2005). Low-molecular-weight diacids are one of the most abundant organic compound classes in  
46 the atmosphere (Kawamura and Ikushima, 1993; Kawamura et al., 1996; Kawamura and Bikkina,  
47 2016). They are primarily derived from incomplete combustion of fossil fuel and biomass burning  
48 (Kawamura and Kaplan, 1987; Falkovich et al., 2005), and secondarily produced in the atmosphere  
49 via photooxidation of unsaturated fatty acids and volatile organic compounds (VOCs) from  
50 biogenic and anthropogenic sources (Kawamura and Gagosian, 1987; Kawamura et al., 1996;  
51 Sempéré and Kawamura, 2003). The ability of organic aerosols to act as cloud condensation nuclei  
52 (CCN) seems to be closely related to their mass-based size distributions (Pradeep Kumar et al.,  
53 2003; Ervens et al., 2007).

54 The increasing atmospheric burden of organic aerosols is associated with natural and  
55 anthropogenic emissions in the continental regions. Organic aerosols are eventually transported to  
56 the oceanic regions. The rapid industrialization in East Asia is expected to have important impact  
57 on global atmospheric chemistry over the next decades (Wang et al., 2013; Tao et al., 2013; Bian et  
58 al., 2014). Large amounts of coal and biomass burning in East Asia add more anthropogenic

59 aerosols altering the aerosol chemical composition in the remote Pacific atmosphere (Mochida et  
60 al., 2007; Miyazaki et al., 2010; Agarwal et al., 2010; Wang et al., 2011; Engling et al., 2013).  
61 Water-soluble diacids and related compounds as well as major ions are previously studied for their  
62 size distributions in remote marine aerosols (Kawamura et al., 2007; Mochida et al., 2007;  
63 Miyazaki et al., 2010), whereas their size-segregated characteristics have not been studied in the  
64 western North Pacific Rim.

65 We collected size-segregated aerosol samples with 9-size ranges in spring 2008 in Cape Hedo,  
66 Okinawa in the western North Pacific Rim. Cape Hedo is located on the northern edge of Okinawa  
67 Island and can serve as a suitable site for the observation of atmospheric transport of East Asian  
68 aerosols with insignificant interference from local emission sources (Takami et al., 2007). The  
69 samples were analyzed for dicarboxylic acids ( $C_2$ - $C_{12}$ ) and related compounds such as  $\omega$ -oxoacids  
70 ( $\omega C_2$ - $\omega C_9$ ), pyruvic acid ( $C_3$ ), and  $\alpha$ -dicarbonyls ( $C_2$ - $C_3$ ) to better understand the sources and  
71 processing of water-soluble organic compounds at this marine receptor site. Size-segregated  
72 samples were also analyzed for water-soluble organic carbon (WSOC), organic carbon (OC), and  
73 major inorganic ions. The role of liquid water content of aerosol in the size distribution of diacids  
74 and related compounds is discussed. The potential factors responsible for their size distributions are  
75 also discussed.

## 76 **2 Materials and method**

### 77 **2.1 Site description and aerosol collection**

78 The geographical location of Okinawa Island (26.87°N and 128.25°E) and its surroundings in East  
79 Asia are shown in Figure 1. Okinawa is located in the outflow region of continental aerosols and on  
80 the pathways to the Pacific. Cape Hedo has been used as a supersite of Atmospheric Brown Clouds  
81 project to study the atmospheric transport of Chinese aerosols and their chemical transformation  
82 during long-range transport from East Asia (Takiguchi et al., 2008; Kunwar and Kawamura, 2014).  
83 The sampling site at Cape Hedo is about 60 m a.s.l.

84 Size-segregated aerosol samples were collected at Cape Hedo Atmospheric and Aerosol  
85 Monitoring Station (CHAAMS) in March 18 to April 13, 2008. This period is characterized by the

86 westerly wind in the lower troposphere, which is the principal process responsible for the transport  
87 of both fossil fuel combustion and biomass burning aerosols in East Asia to the western North  
88 Pacific. 9-Stage Andersen Middle Volume Impactor (Tokyo Dylec Company, Japan; 100 L min<sup>-1</sup>)  
89 was used for the collection of size-segregated samples. The sampler was equipped with quartz fiber  
90 filters (QFF, 80 mm in diameter) that were pre-combusted at 450°C for 6 h in a furnace to eliminate  
91 the adsorbed organic compounds. A total of five sets (OKI-1 to OKI-5) of size-segregated aerosol  
92 samples were collected. Each sample set consists of nine filters for the sizes of <0.43, 0.43-0.65,  
93 0.65-1.1, 1.1-2.1, 2.1-3.3, 3.3-4.7, 4.7-7.0, 7.0-11.3, and >11.3 μm. The filter was placed in a  
94 preheated 50 mL glass vial with a Teflon-lined screw cap and stored in a freezer at the station. The  
95 samples were stored in darkness at -20°C prior to analysis in Sapporo. One set of field blank was  
96 collected by placing a pre-combusted QFF for 30s without sucking air before installing real QFF  
97 into the sampler.

## 98 **2.2 Analytical procedures**

99 Diacids and related compounds were determined by the method of Kawamura and Ikushima (1993),  
100 and Kawamura (1993). Aliquot of the filters was extracted with organic-free ultrapure water  
101 (specific resistivity >18.2 MΩ-cm) under ultrasonication. The extracts were passed through a glass  
102 column packed with quartz wool to remove insoluble particles and filter debris. The extracts were  
103 concentrated using a rotary evaporator under vacuum and derivatized to dibutyl esters and dibutoxy  
104 acetals with 14% BF<sub>3</sub> in *n*-butanol at 100°C. Acetonitrile and *n*-hexane were added into the  
105 derivatized sample and washed with organic-free pure water. The hexane layer was further  
106 concentrated using a rotary evaporator under vacuum and dried to almost dryness by N<sub>2</sub> blowdown  
107 and dissolved in 100 μL of *n*-hexane. Two μL of the sample were injected into a capillary GC  
108 (Hewlett-Packard HP6890) equipped with an FID detector. Authentic diacid dibutyl esters were  
109 used as external standards for the peak identification and quantification. Identifications of diacids  
110 and related compounds were confirmed by GC-mass spectrometry. Recoveries of authentic  
111 standards spiked to a pre-combusted QFF were 85% for oxalic acid (C<sub>2</sub>) and more than 90% for

112 malonic to adipic (C<sub>3</sub>-C<sub>6</sub>) acids. The detection limits of diacids and related compounds were ca.  
113 0.002 ng m<sup>-3</sup>. The analytical errors in duplicate analyses are within 10% for major species.

114 To measure water-soluble organic carbon (WSOC), a punch of 20 mm diameter of each QFF  
115 was extracted with organic-free ultrapure water in a 50 mL glass vial with a Teflon-lined screw cap  
116 under ultrasonication for 15 min. The water extracts were subsequently passed through a syringe  
117 filter (Millex-GV, Millipore; diameter of 0.22 μm). The extract was first acidified with 1.2 M HCl  
118 and purged with pure air in order to remove dissolved inorganic carbon and then WSOC was  
119 measured using a total organic carbon (TOC) analyzer (Shimadzu TOC-V<sub>CSH</sub>) (Miyazaki et al.,  
120 2011). External calibration was performed using potassium hydrogen phthalate before analysis of  
121 WSOC. The sample was measured three times and the average value was used for the calculation of  
122 WSOC concentrations. The analytical error in the triplicate analysis was 5% with a detection limit  
123 of 0.1 μgC m<sup>-3</sup>.

124 Organic and elemental carbon (OC and EC) was determined using a Sunset Lab carbon analyzer  
125 following the Interagency Monitoring of Protected Visual Environments (IMPROVE) thermal  
126 evolution protocol as described by Wang et al. (2005a). A filter disc of 1.5 cm<sup>2</sup> was placed in a  
127 quartz tube inside the thermal desorption chamber of the analyzer and then stepwise heating was  
128 applied. Helium (He) gas was applied in the first ramp and was switched to mixture of He/O<sub>2</sub> in the  
129 second ramp. The evolved CO<sub>2</sub> during the oxidation at each temperature step was measured with  
130 non-dispersive infrared (NDIR) detector system. The detection limits of OC and EC were ca. 0.05  
131 and 0.02 μgC m<sup>-3</sup>, respectively. The analytical errors in the triplicate analysis of the filter sample  
132 were estimated to be 5% for OC and EC. EC was detected only in fine fractions. The concentration  
133 of total carbon (TC) was calculated by summing the concentrations of OC and EC in each size  
134 fraction.

135 For the determination of major ions, a punch of 20 mm diameter of each filter was extracted with  
136 organic-free ultrapure water under ultrasonication. These extracts were filtered through a disc filter  
137 (Millex-GV, Millipore; diameter of 0.22 μm) and injected to ion chromatograph (Compact IC 761;  
138 Metrohm, Switzerland) for measuring MSA<sup>-</sup>, Cl<sup>-</sup>, SO<sub>4</sub><sup>2-</sup>, NO<sub>3</sub><sup>-</sup>, Na<sup>+</sup>, NH<sub>4</sub><sup>+</sup>, K<sup>+</sup>, Ca<sup>2+</sup>, and Mg<sup>2+</sup>  
139 (Boreddy and Kawamura, 2015). Anions were separated on a SI-90 4E Shodex column (Showa

140 Denko; Tokyo, Japan) using a mixture of 1.8 mM Na<sub>2</sub>CO<sub>3</sub> and 1.7 mM NaHCO<sub>3</sub> solution at a flow  
141 rate of 1.2 mL min<sup>-1</sup> as an eluent and 40 mM H<sub>2</sub>SO<sub>4</sub> for a suppressor. A Metrosep C2-150 Metrohm  
142 column was used for cation analysis using a mixture of 4 mM tartaric acid and 1 mM dipicolinic  
143 acid solution as an eluent at a flow rate of 1.0 mL min<sup>-1</sup>. The injected loop volume was 200 µL. The  
144 detection limits for anions and cations were ca. 0.1 ng m<sup>-3</sup>. The analytical error in duplicate analysis  
145 was about 10%.

146 Field blanks were extracted and analyzed like the real samples. However, blank levels were 0.1-  
147 5% of real samples. The reported concentrations of organic and inorganic species were corrected for  
148 the field blanks. All the chemicals including authentic standards were purchased from Wako Pure  
149 Chemical Co. (Japan), except for 14% BF<sub>3</sub>/n-butanol (Sigma-Aldrich, USA).

### 150 **2.3 Backward air mass trajectories and meteorology**

151 The backward trajectories of air masses were computed for the sampling period using the Hybrid  
152 Single-Particle Lagrangian Integrated Trajectory (HYSPPLIT) model 4.0 developed by the National  
153 Oceanic and Atmospheric Administration (NOAA) Air Resources Laboratory (ARL) (Draxler and  
154 Rolph, 2013). The seven-day trajectories at 500 m above the ground level for the samples collected  
155 in Okinawa are shown in Figure 2. Typical air mass trajectories corresponding to 0900 UTC for the  
156 samples collected in Okinawa are shown in Figure S1 in the supporting information.

157 Meteorological data including ambient temperature, relative humidity and wind speed for each  
158 sample period were obtained from Japan Meteorological Agency ([http://www/data/jma.go.jp](http://www.data/jma.go.jp)).  
159 During our campaign, ambient temperature, relative humidity and wind speed ranged from 11.9 to  
160 26.6 °C (ave. 20.0±2.6 °C), 43.0 to 91.0% (ave. 70.0±12.0%), 0.10 to 10.2 m s<sup>-1</sup> (ave. 3.73±1.99 m  
161 s<sup>-1</sup>), respectively. The seven-day trajectories along with the meteorological data including  
162 precipitation and downward solar radiation flux are shown in Figure S2.

### 163 **2.4 Estimation of liquid water content (LWC) of aerosol**

164 LWC of aerosol was calculated for the size-segregated samples collected in Okinawa Island using  
165 the ISORROPIA II model (Fountoukis and Nenes, 2007). ISORROPIA II is a computationally  
166 efficient and rigorous thermodynamic equilibrium model that exhibits robust and rapid convergence

167 under all aerosol types with high computational speed (Nenes et al., 1998). ISORROPIA II implies  
168 the Zdanovskii-Stokes-Robinson equation and treats only the thermodynamics of  $K^+$  - $Ca^{2+}$  - $Mg^{2+}$  -  
169  $NH_4^+$  - $Na^+$  - $SO_4^{2-}$  - $NO_3^-$  - $Cl^-$  - $H_2O$  aerosol system to estimate the LWC. Therefore, the measured  
170 organic species such as diacids and related compounds are not included in ISORROPIA II. The  
171 model was run as “reverse problem”, in which temperature, relative humidity and aerosol phase  
172 concentrations of water-soluble inorganic ions were used as input for the estimation of aerosol  
173 LWC.

### 174 **3 Results and discussion**

#### 175 **3.1 Size-segregated aerosol chemical characteristics**

176 We use 2.1  $\mu m$  as a split diameter between the fine and coarse mode particles. Table 1 presents the  
177 concentrations of inorganic and carbonaceous species in the fine and coarse mode aerosols.  
178 Abundances of organic matter (OM) in the atmosphere are generally estimated by multiplying the  
179 measured OC mass concentrations with the conversion factor of 1.6 for urban aerosols and 2.1 for  
180 aged aerosols (Turpin and Lim, 2001). CHAAMS is located in the outflow region of East Asian  
181 aerosols and local anthropogenic activities are insignificant. Because the aerosols reaching to  
182 Okinawa are subjected to undergo the atmospheric oxidation during the long-range transport, the  
183 fraction of oxygenated organic species is often high (Takami et al., 2007; Irei et al., 2014; Kunwar  
184 and Kawamura, 2014). Therefore, we used the conversion factor of 2.1, instead of 1.6 for  
185 calculation of OM.

186 OM was enriched in fine size fractions than the coarse size fractions (Table 1). The elevated  
187 level of OM in fine fractions in Okinawa suggests a substantial contribution of organic aerosols  
188 primarily from combustion sources and secondarily from photochemical processes during long-  
189 range atmospheric transport. The OM in fine mode aerosol in Okinawa may consist of oxygenated  
190 organic compounds such as diacids,  $\omega$ -oxoacids and  $\alpha$ -dicarbonyls. Okinawa was strongly affected  
191 by long-range transport of continental air masses from Siberia and Mongolia as well as North China  
192 and Korea (Figure 2). It is difficult to specify the source regions of air masses for each sample set  
193 because the sampling duration was 3-5 days. Each sample contains mixed continental and oceanic  
194 air masses. Precipitation may have an insignificant effect on the transport of pollutants from the

195 source region to Okinawa because air masses were not experienced serious precipitation events  
196 during the transport (Figure S2a).

197 Sulfate is the most abundant anion in fine mode whereas chloride is the dominant anion in coarse  
198 mode. The cation budget is largely controlled by ammonium in fine mode whereas sodium is the  
199 most abundant cation in coarse mode. The high abundance of  $\text{SO}_4^{2-}$  in fine particles suggests a  
200 significant contribution of anthropogenic sources including industrial emissions in East Asia via  
201 long-range transport of aerosols over the western North Pacific Rim.  $\text{SO}_4^{2-}$  is an anthropogenic  
202 tracer of industrial activities whereas  $\text{NH}_4^+$  is the secondary product of  $\text{NH}_3$  that is largely derived  
203 from the agricultural usage of nitrogen-based fertilizers (Pakkanen et al., 2001) and volatilization  
204 from soils and livestock waste in East Asia (Huang et al., 2006). The dominant presences of  $\text{Na}^+$   
205 and  $\text{Cl}^-$  in coarse mode suggest a substantial contribution from sea salt.  $\text{Na}^+$  and  $\text{Cl}^-$  are emitted  
206 from the ocean surface as relatively larger particles. Substantial amount of  $\text{NO}_3^-$  was detected in  
207 coarse mode, suggesting a formation of  $\text{Ca}(\text{NO}_3)_2$  or  $\text{NaNO}_3$  in coarse fractions through the reactive  
208 adsorption of gaseous  $\text{HNO}_3$  onto pre-existing alkaline particles.

209 The molecular distributions of detected diacids and related compounds in size-segregated  
210 aerosols are shown in Figure 3. Table 2 presents the summarized concentrations of those  
211 compounds in fine and coarse modes. Oxalic acid ( $\text{C}_2$ ) was found as the most abundant diacid  
212 followed by malonic ( $\text{C}_3$ ) and succinic ( $\text{C}_4$ ) acids in all size-segregated aerosols. The predominance  
213 of  $\text{C}_2$  in size-segregated aerosols is due to the fact that it can be secondarily produced by the  
214 photooxidation of anthropogenic and biogenic organic precursors in gas and aqueous-phase  
215 (Kawamura and Sakaguchi, 1999; Warneck, 2003; Carlton et al., 2006).  $\text{C}_2$  can also be produced  
216 primarily from fossil fuel combustion (Kawamura and Kaplan, 1987) and biomass burning (Kundu  
217 et al., 2010) in East Asia and long-range transported to Okinawa.

218 Phthalic (Ph) and adipic ( $\text{C}_6$ ) acids are the next abundant diacids whereas ketomalonic acid ( $\text{kC}_3$ )  
219 is more abundant than  $\text{C}_6$  diacid in the size ranges of 0.43-0.65  $\mu\text{m}$  to 0.65-1.1  $\mu\text{m}$  (Figure 3). Ph  
220 and  $\text{C}_6$  diacids originate from various anthropogenic sources and thus they can be used as  
221 anthropogenic tracers. Ph primarily originates from coal burning and vehicular emission whereas  
222 photooxidation of aromatic hydrocarbons such as naphthalene and o-xylene derived from

223 incomplete combustion of fossil fuel from Ph via secondary processes (Kawamura and Kaplan,  
224 1987). Moreover, abundant presence of Ph may also be caused by enhanced emission of phthalates  
225 from plastics used in heavily populated and industrialized regions in China and the subsequent  
226 long-range atmospheric transport to Okinawa. Phthalic acid esters are used as plasticizers in resins  
227 and polymers (Simoneit et al., 2005). They can be released into the air by evaporation because they  
228 are not chemically bonded to the polymer. Kawamura and Usukura (1993) reported that C<sub>6</sub> diacid is  
229 an oxidation product through the reaction of cyclohexene with ozone (O<sub>3</sub>). The high abundances of  
230 Ph and C<sub>6</sub> diacids in Okinawa suggest a significant influence of anthropogenic sources in East Asia  
231 via long-range transport of aerosols over the western North Pacific Rim.

232 Azelaic acid (C<sub>9</sub>) is more abundant than adjacent suberic (C<sub>8</sub>) and decanedioic (C<sub>10</sub>) acids in all  
233 the size-segregated aerosols (Figure 3 and Table 2). Kawamura and Gagosian (1987) proposed that  
234 C<sub>9</sub> is a photooxidation product of biogenic unsaturated fatty acids such as oleic acid (C<sub>18:1</sub>)  
235 containing a double bond at C-9 position. Unsaturated fatty acids can be emitted from sea surface  
236 microlayers and from local vegetation in Okinawa (Kunwar and Kawamura, 2014). Moreover,  
237 Okinawa was affected by long-range transport of air masses from Siberia and Mongolia as well as  
238 North China and Korea (Figure 2). Such continental air masses can also deliver C<sub>9</sub> via atmospheric  
239 processing of unsaturated fatty acids during long-range transport. The abundant presence of C<sub>9</sub>  
240 indicates that atmospheric oxidation of unsaturated fatty acids also occurs in Okinawa aerosols  
241 during long-range transport.  $\omega$ -Oxocarboxylic acids and  $\alpha$ -dicarbonyls were detected in the  
242 Okinawa aerosols. Glyoxylic acid ( $\omega$ C<sub>2</sub>) was identified as the most abundant  $\omega$ -oxoacid whereas  
243 glyoxal (Gly) was more abundant than methylglyoxal (MeGly) in all the sizes.  $\omega$ C<sub>2</sub> and Gly are the  
244 oxidation product of several anthropogenic and biogenic VOCs and primary generated by fossil fuel  
245 combustion and biomass burning (Zimmermann and Poppe, 1996; Volkamer et al., 2001), and are  
246 further oxidized to C<sub>2</sub> diacid (Myriokefalitakis et al., 2011). The predominance of  $\omega$ C<sub>2</sub> and Gly  
247 indicates their importance as key precursors of C<sub>2</sub> in Okinawa aerosols.

### 248 3.2 Inorganic species



249 The particle size distributions of major ions are shown in Figure 4. Pearson correlation coefficients  
250 ( $r$ ) among the measured ions in different size modes are given in Table 3.  $\text{Na}^+$  and  $\text{Cl}^-$  are mainly  
251 derived from the ocean surface as sea salt particles in the marine atmosphere (Kumar et al., 2008;  
252 Geng et al., 2009). The size distributions of  $\text{Na}^+$  and  $\text{Cl}^-$  were found to be bimodal with two peaks  
253 in coarse mode (Figure 4a and b). Their peaks at 2.1-3.3 or 3.3-4.7  $\mu\text{m}$  and at  $>11.3 \mu\text{m}$  suggest that  
254 they are of marine origin due to bubble bursting of surface seawater. Andreas (1998) suggested that  
255 the sea spray fall into two types that are defined as film and jet bubbles; film bubbles correspond to  
256 the size of 0.5-5  $\mu\text{m}$  whereas jet bubbles produce the size of 5-20  $\mu\text{m}$ . Their coarse mode peaks at  
257 2.1-3.3  $\mu\text{m}$  or 3.3-4.7 and  $>11.3 \mu\text{m}$  in Okinawa aerosols were associated with film and jet bubbles.  
258 We found that size distribution of  $\text{Mg}^{2+}$  is similar to those of  $\text{Na}^+$  and  $\text{Cl}^-$  with a significant positive  
259 correlation to coarse mode  $\text{Na}^+$  and  $\text{Cl}^-$  ( $r = 0.98$ ), suggesting their similar origin and sources.

260 A high concentration of  $\text{Ca}^{2+}$  in coarse mode particles demonstrates its contributions from soil  
261 dust (Kerminen et al., 1997a; Tsai and Chen, 2006). A lifting of soil dust in continental sites  
262 followed by subsequent long-range atmospheric transport to remote marine site is also proposed as  
263 an important source of  $\text{Ca}^{2+}$  (Wang et al., 2005b).  $\text{Ca}^{2+}$  showed unimodal distribution with a peak at  
264 either 2.1-3.3 or 3.3-4.7  $\mu\text{m}$  (Figure 4c). The coarse mode  $\text{Ca}^{2+}$  is mostly derived from crustal  
265  $\text{CaCO}_3$ , which heterogeneously reacts with acidic gases ( $\text{HNO}_3$  and  $\text{SO}_2$ ) (Kerminen et al., 1997a).  
266 This formation mechanism is further supported by a strong correlation of coarse mode  $\text{Ca}^{2+}$  with  
267  $\text{NO}_3^-$  ( $r = 0.98$ ). There is no correlation between  $\text{Ca}^{2+}$  and  $\text{Na}^+$  or  $\text{Cl}^-$  ( $r = -0.12$  or  $-0.27$ ), revealing  
268 that sea salt contribution of  $\text{Ca}^{2+}$  is negligible in Okinawa aerosols. This result suggests that long-  
269 range transport of soil dust is an important contributor of  $\text{Ca}^{2+}$  in the marine aerosols from the  
270 western North Pacific Rim.

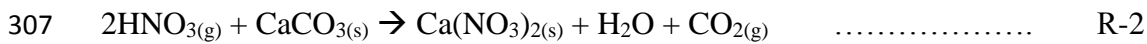
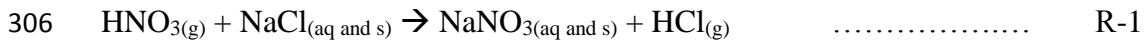
271 There is natural limestone caves formed by elevated coral reefs in Okinawa Island. Although  
272 local limestone dust may also be re-suspended to the atmosphere by wind (Shimada et al., 2015),  
273 the local dust contribution to the ambient level of  $\text{Ca}^{2+}$  in Okinawa may be small. This  
274 interpretation can be supported by the fact that  $\text{Ca}^{2+}$  peaked in lower coarse size range of 2.1-3.3 or  
275 3.3-4.7  $\mu\text{m}$ . It has been suggested that  $\text{Ca}^{2+}$  is likely associated with upper coarse size range when  
276 the contribution of locally produced soil particles is significant (Bian et al., 2014). Smaller coarse

277 mode  $\text{Ca}^{2+}$  is likely associated with long-range transported Asian dust to Okinawa. Moreover,  
278 concentrations of  $\text{Ca}^{2+}$  in coarse mode were found to be much higher in OKI-1 ( $0.51 \mu\text{g m}^{-3}$ ) and  
279 OKI-2 ( $0.60 \mu\text{g m}^{-3}$ ) than that OKI-5 sample ( $0.15 \mu\text{g m}^{-3}$ ). Backward trajectories also indicated  
280 that the air masses originated from Mongolia and Siberia were transported to Okinawa during the  
281 collection of OKI-1 and OKI-2 samples whereas OKI-5 sample has an influence of marine air  
282 masses. Such air mass origin again indicates a long-range transport of Asian dust from East Asia to  
283 the western North Pacific.

284 Potassium is enriched in biomass burning aerosols and therefore its abundances in fine particles  
285 can serve as a diagnostic tracer of biomass burning (Yamasoe et al., 2000). Moreover, contributions  
286 of  $\text{K}^+$  from sea salt and dust sources are highly variable in regional case studies with its dominance  
287 in coarse mode particles. Fresh biomass burning particles mostly reside in the condensation mode at  
288  $0.1\text{-}0.5 \mu\text{m}$  in diameter (Kaufman and Fraser, 1997; Kleeman and Cass, 1999). A unimodal size  
289 distribution of  $\text{K}^+$  was observed in most sample sets (OKI-1 to OKI-4) with a peak at  $0.65\text{-}1.1 \mu\text{m}$   
290 in diameter (Figure 4e). The peak of  $\text{K}^+$  at  $0.65\text{-}1.1 \mu\text{m}$  suggests that biomass burning particles  
291 emitted in East Asia might have undergone a growth to a relatively large size by absorbing water  
292 vapor from the atmosphere during long-range transport to Okinawa. This interpretation is supported  
293 by the fact that  $\text{K}^+$  showed a positive correlation with LWC ( $r = 0.83$ ) in fine mode. The fine mode  
294 nss- $\text{K}^+$  accounted for 95% of total  $\text{K}^+$  in OKI-2 sample set and 88% of that in OKI-3 sample set  
295 when air masses are coming from Siberia and Mongolia as well as North China. The abundant  
296 presence of fine mode nss- $\text{K}^+$  in the OKI-2 and OKI-3 samples further indicates a long-range  
297 atmospheric transport of biomass burning aerosols from the Asian continent to the western North  
298 Pacific Rim.

299  $\text{NO}_x$  is a precursor of  $\text{NO}_3^-$ , which can be converted to  $\text{HNO}_3$  and then react with  $\text{NH}_3$  to form  
300  $\text{NH}_4\text{NO}_3$ . A unimodal size distribution of  $\text{NO}_3^-$  was observed with a peak at  $2.1\text{-}3.3$  or  $3.3\text{-}4.7 \mu\text{m}$   
301 in diameter (Figure 4f). It should also be noted that the  $\text{NO}_3^-$  concentration in coarse mode is much  
302 higher than that in fine mode (Table 1). This result suggests that either dust or sea salt particle is the  
303 source of coarse mode  $\text{NO}_3^-$  in Okinawa. Coarse mode  $\text{NO}_3^-$  is produced by heterogeneous reaction

304 of gaseous  $\text{NO}_2$  or  $\text{HNO}_3$  with alkaline metals such as  $\text{Na}^+$  and  $\text{Ca}^{2+}$  as shown in Reactions 1 and 2  
 305 (Kouyoumdjian and Saliba, 2006; Seinfeld and Pandis, 2006).



308 As discussed earlier, the air masses originated from Siberia are transported over Mongolia and  
 309 North China. Asian dust can be transported from the Asian continent to Okinawa. Therefore, it is  
 310 possible that the gaseous  $\text{HNO}_3$  might already have reacted with  $\text{CaCO}_3$  (mineral dust particle) to  
 311 form  $\text{NO}_3^-$  before arriving to Okinawa through R-2. We found that coarse mode  $\text{Na}^+$ , which is  
 312 derived from sea salts, is negatively correlated ( $r = -0.30$ ) with coarse mode  $\text{NO}_3^-$ . Although this  
 313 correlation is not significant ( $p = 0.51$ ), the negative correlation may indicate some reactive loss of  
 314  $\text{NO}_3^-$  from sea salt particles in coarse mode in Okinawa.  $\text{NO}_3^-$  peaked at the same particle size of  
 315  $\text{Ca}^{2+}$ . Therefore,  $\text{NO}_3^-$  in Okinawa coarse mode aerosols was probably resulted from the uptake of  
 316  $\text{HNO}_3$  gas by soil dust particles enriched with  $\text{Ca}^{2+}$  via heterogeneous reaction near the source  
 317 regions. This process is further supported by a good correlation between  $\text{NO}_3^-$  and  $\text{Ca}^{2+}$  ( $r = 0.98$ ) in  
 318 coarse mode.

319 The particle size distributions of  $\text{SO}_4^{2-}$ , which is a major source of acid deposition (Pakkanen et  
 320 al., 2001), have been the subject of numerous studies in the past few decades (Huang et al., 2006;  
 321 Kouyoumdjian and Saliba, 2006). Condensation mode  $\text{SO}_4^{2-}$  arises from gas-phase oxidation of  $\text{SO}_2$   
 322 followed by gas-to-particle conversion whereas fine mode  $\text{SO}_4^{2-}$  is formed through aqueous-phase  
 323 oxidation of  $\text{SO}_2$  in aerosols and cloud droplets (Seinfeld and Pandis, 1998).  $\text{SO}_4^{2-}$  on coarse mode  
 324 can be attributed to a combination of sulfate and heterogeneous reactions of  $\text{SO}_2$  on soil dust or sea  
 325 salt particles (Seinfeld and Pandis, 1998; Pakkanen et al., 2001). A unimodal size distribution of  
 326  $\text{SO}_4^{2-}$  was observed with a peak at 0.65-1.1  $\mu\text{m}$  (Figure 4g). Gao et al. (2012) suggested that in-  
 327 cloud process produces  $\text{SO}_4^{2-}$  as larger particles by aqueous-phase oxidation of  $\text{SO}_2$  in cloud  
 328 droplets. Therefore, the peak of  $\text{SO}_4^{2-}$  at 0.65-1.1  $\mu\text{m}$  in Okinawa may be involved with aqueous-  
 329 phase oxidation of  $\text{SO}_2$  in aerosols.

330 Size distribution of methanesulfonate ( $\text{MSA}^-$ ) is similar to that of  $\text{SO}_4^{2-}$  (Figure 4i) in Okinawa.  
 331  $\text{MSA}^-$  showed a strong correlation with  $\text{SO}_4^{2-}$  ( $r = 0.89$ ) in fine mode, suggesting that  $\text{MSA}^-$  should

332 have similar origin with  $\text{SO}_4^{2-}$  in fine mode. Although  $\text{MSA}^-$  is produced by gas-to-particle  
333 conversion via the oxidation of dimethyl sulfide (DMS) emitted from the ocean (Quinn et al., 1993;  
334 Kerminen et al., 1997b), there is some indirect evidence that liquid-phase production might also be  
335 possible (Jefferson et al., 1998). Biomass burning also produces DMS in the atmosphere (Meinardi  
336 et al., 2003; Geng and Mu, 2006).  $\text{MSA}^-$  showed high correlation with  $\text{K}^+$  or  $\text{NH}_4^+$  ( $r = 0.92$ ) in fine  
337 mode, indicating that an enhanced emission of DMS from biomass burning followed by the  
338 subsequent oxidation during long-range transport may have contributed significantly to fine mode  
339  $\text{MSA}^-$  in Okinawa. Moreover,  $\text{MSA}^-$  can also be produced in fine mode by the oxidation of DMS  
340 that is emitted from marine phytoplankton in the surrounding ocean. It is noteworthy that East  
341 Asian aerosols travelled over the marine regions including the East China Sea, Sea of Japan and  
342 Pacific Ocean during long-range atmospheric transport. The size distribution of  $\text{MSA}^-$  observed  
343 over Okinawa is consistent with previous studies from the China Sea by Gao et al. (1996), who  
344 suggested that MSA is produced through the oxidation of S-containing species in the marine  
345 atmosphere.

346  $\text{NH}_4^+$  in the Okinawa aerosols shows a unimodal size distribution with a peak at 0.65-1.1  $\mu\text{m}$   
347 (Figure 4h), indicating that  $\text{NH}_4^+$  is mainly formed by gas-to-particle conversion via the reaction  
348 with  $\text{H}_2\text{SO}_4$  and  $\text{HNO}_3$ . Interestingly, the size distribution of  $\text{NH}_4^+$  is similar to that of  $\text{SO}_4^{2-}$  and  
349 diacids such as oxalic acid (Figure 4g and 5a). We also found a strong correlation between  $\text{SO}_4^{2-}$   
350 and  $\text{NH}_4^+$  on fine mode ( $r = 0.99$ ). Ion balance calculations are commonly used to evaluate acid-  
351 base balance of aerosol particles. Average equivalent ratios of total cations ( $\text{Na}^+$ ,  $\text{NH}_4^+$ ,  $\text{K}^+$ ,  $\text{Mg}^{2+}$   
352 and  $\text{Ca}^{2+}$ ) to anions ( $\text{Cl}^-$ ,  $\text{NO}_3^-$  and  $\text{SO}_4^{2-}$ ) in fine fractions varied from 0.75 for the size bin of 0.65-  
353 1.1  $\mu\text{m}$  to 0.86 for the size bin of 1.1-2.1  $\mu\text{m}$ , indicating that fine mode aerosols in Okinawa were  
354 apparently acidic.

355  $\text{NH}_3$  is an alkaline gas that neutralizes the acidic particles in the atmosphere. Kerminen et al.  
356 (1997a) proposed that particulate  $\text{NH}_4^+$  is secondarily formed via heterogeneous reactions of  
357 gaseous  $\text{NH}_3$  with acidic species ( $\text{H}_2\text{SO}_4$  and  $\text{HNO}_3$ ). The reaction of  $\text{NH}_3$  with  $\text{H}_2\text{SO}_4$  is favored  
358 over its reaction with  $\text{HNO}_3$ . The average  $\text{NH}_4^+/\text{SO}_4^{2-}$  equivalent ratios in fine mode particles in  
359 Okinawa varied from 0.36 for the size bin of 1.1-2.1  $\mu\text{m}$  to 0.81 for the size bin of 0.43-0.65  $\mu\text{m}$ ,

360 indicating that  $\text{NH}_3$  was not abundant enough to neutralize all  $\text{SO}_2$ . The aerosol chemical  
361 composition data obtained from the ISORROPIA II model revealed that significant amounts of  
362  $\text{SO}_4^{2-}$ ,  $\text{HSO}_4^-$  and  $\text{NH}_4^+$  in fine mode were present in liquid-phase whereas  $\text{SO}_4^{2-}$  and  $\text{NO}_3^-$  were  
363 mainly present as solid-phase in the coarse mode aerosols in the forms of  $\text{CaSO}_4$  and  $\text{Ca}(\text{NO}_3)_2$ ,  
364 respectively. Interestingly, the average  $\text{NH}_4^+/\text{SO}_4^{2-}$  equivalent ratios in coarse mode particles ranged  
365 from 0.01 for the size bin  $>11.3 \mu\text{m}$  to 0.09 for the size bins of 2.1-3.3 and 3.3-4.7  $\mu\text{m}$ , suggesting  
366 that coarse mode aerosols in Okinawa were also  $\text{NH}_4^+$ -poor. This result further indicates that there  
367 was not enough  $\text{NH}_3$  to neutralize  $\text{HNO}_3$ , and thus shortfall of  $\text{NH}_3$  may be the restrictive factor for  
368 the formation of  $\text{NH}_4\text{NO}_3$  in Okinawa aerosols. Therefore,  $\text{NO}_3^-$  reacts with coarse particles that  
369 contain alkaline species ( $\text{Ca}^{2+}$ ) in Okinawa aerosols.

370 The size distribution of  $\text{SO}_4^{2-}$  depends on the concentration of  $\text{NH}_4^+$ , richness of  $\text{NH}_3$  in the air,  
371 and the presence of coarse mode particles.  $\text{SO}_4^{2-}$  and  $\text{NH}_4^+$  often coexist in fine mode because  
372  $\text{H}_2\text{SO}_4$  condenses on this mode as fine particles that have more surface area (Jacobson, 2002).  
373 Although  $\text{NH}_3$  was not abundant enough to neutralize all  $\text{SO}_4^{2-}$ , most of  $\text{SO}_4^{2-}$  might be neutralize  
374 by  $\text{NH}_3$  in fine mode. Hence,  $\text{SO}_4^{2-}$  is enriched in fine mode rather than being associated with dust  
375 particles. An enrichment of  $\text{NO}_3^-$  in the dust fraction in our study is supported by the laboratory  
376 studies of Hanisch and Crowley (2001a, 2001b), who found a large and irreversible uptake between  
377  $\text{HNO}_3$  and various authentic dust samples including samples from Chinese dust region.

### 378 3.3 Water-soluble organic carbon (WSOC) and organic carbon (OC)

379 The mass-based size distribution of WSOC is characterized by a major peak at 0.65-1.1  $\mu\text{m}$  in  
380 fine mode and by a small peak at 3.3-4.7  $\mu\text{m}$  in coarse mode (Figure 6a and Table 1). Huang et al.  
381 (2006) observed that fine mode WSOC was primarily derived from combustion sources and  
382 secondarily produced in the atmosphere by the photochemical oxidation of VOCs. The WSOC  
383 concentrations showed a strong correlation with fine mode  $\text{SO}_4^{2-}$  ( $r = 0.96$ ). Because production of  
384  $\text{SO}_4^{2-}$  is closely linked to photochemical activity, this result suggests an important secondary  
385 production of WSOC in fine mode particles during long-range atmospheric transport from East  
386 Asia. WSOC concentrations also showed high correlation with  $\text{K}^+$  ( $r = 0.93$ ) and  $\text{NH}_4^+$  ( $r = 0.91$ ) in  
387 fine mode. This result suggests that direct emission from biomass burning or fast oxidation of

388 biomass burning-derived precursors significantly contributes to the formation of fine mode WSOC  
389 in Okinawa aerosols during long-range transport.

390 The mass-size distribution pattern of OC is similar to that of WSOC with a major peak in the  
391 size range of 0.65-1.1  $\mu\text{m}$  whereas a small peak was appeared in the size range of 3.3-4.7  $\mu\text{m}$  in  
392 diameter (Figure 6b). Primary emission from biomass burning and/or photooxidation of biomass  
393 burning derived precursors might be a dominant source of fine mode OC in Okinawa aerosols. This  
394 interpretation is supported by the fact that OC showed a strong correlation ( $r = 0.95$ ) with  $\text{K}^+$  in fine  
395 mode. The fine mode OC showed significant positive correlations with  $\text{SO}_4^{2-}$  ( $r = 0.93$ ) and  $\text{NH}_4^+$   
396 (0.91), suggesting a secondary photochemical formation of OC in fine mode of Okinawa aerosols.

397 A significant portion of OC may be oxidized to WSOC during the atmospheric transport from  
398 East Asia to the western North Pacific. The mass ratio of WSOC/OC has been proposed as a  
399 measure of photochemical processing or aging of organic aerosols especially in long-range  
400 transported aerosols (Aggarwal and Kawamura, 2009). The WSOC/OC ratios varied from 0.51-0.76  
401 with an average of  $0.67 \pm 0.09$  in the fine mode and 0.43-0.63 with an average of  $0.55 \pm 0.09$  in the  
402 coarse mode. The higher WSOC/OC ratio in fine mode suggests that organics are significantly  
403 subjected to photochemical processing in fine aerosols during long-range transport from the Asian  
404 continent to Okinawa than coarse mode aerosols.

405 Source contributions and secondary processes that may convert VOCs to amore soluble forms on  
406 the surface area of fine particles could cause higher WSOC/OC ratios in fine mode. Biomass  
407 burning-derived OC is highly water-soluble and usually resides in fine mode whereas coarse mode  
408 OC contains high molecular weight organic compounds emitted by soil resuspension and emissions  
409 of pollens and fungal spores, which are less water-soluble (Wang et al., 2011; Mkoma et al., 2013).  
410 Biomass burning significantly contributed to fine mode WSOC in Okinawa as discussed above.  
411 Moreover, accumulation of gas-phase precursors of WSOC may occur preferentially in the particle  
412 size with the greatest surface area (Kanakidou et al., 2005). It has been proposed that fine particles  
413 offer more surface area and thus reaction rate is more on the surface of fine particles than coarse  
414 particles (Kanakidou et al., 2005). The higher WSOC/OC ratio in fine particles than coarse particles

415 has also been observed in long-range transported East Asian aerosols over Northern Japan (Agarwal  
416 et al., 2010).

417 The WSOC/OC ratio in fine mode showed a weak positive correlation with downward solar  
418 radiation flux ( $r = 0.39$ ). This weak correlation is probably due to the fact that fine mode WSOC  
419 can be produced in aqueous-phase of aerosols during long-range transport. Based on the year round  
420 measurements of TSP aerosols from Okinawa Island, Kunwar and Kawamura (2014) documented  
421 higher WSOC/OC ratio in winter (ave. 0.60) and spring (ave. 0.45) than summer (ave. 0.28). These  
422 observations demonstrate that WSOC can be produced from OC under weak solar radiation  
423 condition on the transport pathway from the source region to Okinawa possibly via aqueous-phase  
424 processing.

425 Calculated LWC for each sample from Okinawa and average LWC in size-segregated aerosols  
426 are shown in Figure 7. The highest LWC was found at the size of 0.65-1.1  $\mu\text{m}$  in the fine mode in  
427 Okinawa samples. WSOC can also contribute to aerosol LWC although their ability to absorb water  
428 is significantly less than that of inorganics (Ansari and Pandis, 2000; Speer et al., 2003; Engelhart et  
429 al., 2011). Moreover, organic species are not taken into account in ISORROPIA II for the  
430 calculation of LWC. It is noteworthy that WSOC/OC ratio and LWC in fine mode significantly  
431 correlate with  $r = 0.87$  whereas negative correlation was found in coarse mode ( $r = -0.19$ ),  
432 suggesting a possible production of WSOC from OC in aerosol aqueous-phase in fine mode of  
433 Okinawa aerosols. There may also be another important sources of fine mode WSOC in Okinawa  
434 aerosols such as primary emission from biomass burning and secondary formation via gas-phase  
435 photochemical reactions during long-range atmospheric transport (Hagler et al., 2007; Lim et al.,  
436 2010). This result may indicate that shorter-chain diacids and related polar compounds can  
437 contribute more to fine mode WSOC via oxidation of various organic precursors during long-range  
438 transport (Carlton et al., 2007; Kawamura et al., 2005, 2007; Miyazaki et al., 2010).

### 439 **3.4 Dicarboxylic acids and related compounds**

440 The size distributions of selected diacids and related compounds are shown in Figure 5. Based on  
441 the sources and formation processes, their size distributions fall into two groups: a group with a  
442 dominant fine mode and a group with a dominant coarse mode as discussed in the ensuing sections.

### 443 3.4.1 C<sub>2</sub>, ωC<sub>2</sub>, Gly, Ph and benzoic acid

444 The first group, including C<sub>2</sub>, ωC<sub>2</sub>, Gly, Ph and benzoic acid, showed the similar size distributions  
445 with maxima in fine mode. C<sub>2</sub> showed a peak at 0.65-1.1 μm in fine mode (Figure 5a). The size  
446 distribution of C<sub>2</sub> in Okinawa is different from that observed off the coast of East Asia by Mochida  
447 et al. (2003a, 2007), who found a strong bimodal pattern of C<sub>2</sub> with a peak in the coarse mode. They  
448 suggested that the coarse mode peak of C<sub>2</sub> was emerged by the uptake of gaseous diacids or  
449 heterogeneous oxidations of organic precursors on the dust and sea salt particles during long-range  
450 transport. The unimodal distribution of C<sub>2</sub> in Okinawa with maxima in fine mode suggests that the  
451 heterogeneous uptake of C<sub>2</sub> on dust and sea-salt particles did not occur.

452 The condensation mode of C<sub>2</sub> is likely produced photochemically in the gas-phase followed by  
453 condensation onto pre-existing particles at 0.1-0.5 μm (Huang et al., 2006). The fine mode peak of  
454 C<sub>2</sub> at the size of 0.65-1.1 μm in Okinawa aerosols suggests a preferential production of C<sub>2</sub> via the  
455 oxidation of precursors in aerosol aqueous-phase during long-range atmospheric transport. We  
456 found that size distribution of C<sub>2</sub> diacid is similar to that of SO<sub>4</sub><sup>2-</sup> (Figure 4g and 5a), suggesting a  
457 secondary formation of C<sub>2</sub> possibly in aerosol aqueous-phase. The good correlations of C<sub>2</sub> with  
458 SO<sub>4</sub><sup>2-</sup> ( $r = 0.92$ ) and NH<sub>4</sub><sup>+</sup> (0.89) in fine mode further supports that C<sub>2</sub> is a secondary photochemical  
459 product. Fine mode C<sub>2</sub> can also be produced primarily from fossil fuel combustion and biomass  
460 burning in East Asia and long-range transported to Okinawa. C<sub>2</sub> diacid showed a significant  
461 positive correlation with fine mode K<sup>+</sup> ( $r = 0.85$ ), indicating that biomass burning contributed  
462 significantly to fine mode C<sub>2</sub> in Okinawa aerosols.

463 Lim et al. (2005) and Legrand et al. (2007) reported the formation of diacids in aqueous-phase.  
464 Here we investigate the impact of LWC on the formation of diacids in Okinawa aerosols. LWC of a  
465 particle can influence the production of C<sub>2</sub> via the changes in gas/particle partitioning of organic  
466 precursors and subsequent heterogeneous reaction in aerosol aqueous-phase. A strong positive  
467 correlation ( $r = 0.92$ ) of C<sub>2</sub> with LWC was found in fine mode whereas the correlation was negative  
468 in coarse mode ( $r = -0.29$ ), indicating a possible aqueous-phase production of C<sub>2</sub> via the oxidation  
469 of C<sub>2</sub> precursors in fine mode. Several secondary formation pathways are known to C<sub>2</sub> in  
470 atmospheric aerosols. C<sub>2</sub> is produced by the decay of its higher homologues (C<sub>3</sub>-C<sub>5</sub> diacids) or



471 oxidation of unsaturated fatty acids such as oleic acid ( $C_{18:1}$ ) followed by the degradation to shorter-  
472 chain diacids in aqueous-phase (Kawamura and Ikushima, 1993; Kawamura and Sakaguchi, 1999;  
473 Pavuluri et al., 2015).  $C_2$  can also be produced by the aqueous-phase oxidation of  $\omega C_2$ , which can  
474 be formed by aqueous oxidation of Gly and MeGly produced by the oxidation of various VOCs  
475 including toluene, ethene and isoprene (Zimmermann and Poppe, 1996; Volkamer et al., 2001; Lim  
476 et al., 2005; Carlton et al., 2006; Ervens et al., 2008).

477 The scatter plots of  $C_2$  with  $C_3$ - $C_5$  diacids in fine and coarse modes are shown in Figure S3. The  
478 robust correlations of  $C_2$  with  $C_3$ - $C_5$  diacids ( $r = 0.89$ - $0.92$ ) were found in fine mode, indicating that  
479 they might have similar sources and origin or  $C_2$  may be produced via the decay of its higher  
480 homologues ( $C_3$ - $C_5$  diacids) during long-range transport. The differences in the slopes of linear  
481 regression of  $C_2$  with  $C_3$  and  $C_4$  diacids between fine and coarse modes are not significant but  
482 slopes are slightly higher in fine mode than the coarse mode (Figure S3a-d and Table S1).  
483 Interestingly, significantly higher slope was observed for regression line between  $C_2$  and glutaric  
484 ( $C_5$ ) acid in fine mode than coarse mode (Figure S3e-f and Table S1). It is also noteworthy that the  
485 slope of regression line of  $C_2$  with  $C_5$  diacid is significantly higher than that for  $C_3$  and  $C_4$  diacids in  
486 fine mode (Figure S3a, c, e and Table S2). These results indicate that fine mode oxalic acid may be  
487 produced from oxidation of glutaric acid during long-range transport via succinic and malonic acids  
488 as intermediates. The laboratory studies of Hatakeyama et al. (1985) and Kalberer et al. (2010) have  
489 documented that glutaric acid is produced by the oxidation of cyclohexene by  $O_3$ , which can be  
490 further oxidized in aqueous-phase to result in oxalic acid (Kawamura and Sakaguchi, 1999;  
491 Legrand et al., 2007). This interpretation is further supported by the fact that  $C_3$ - $C_5$  diacids were  
492 enriched in the fine mode of most samples (Figure 5b-d) and showed good correlations with LWC  
493 ( $r = 0.82$ - $0.89$ ) possibly due to the enhanced secondary production by the oxidation of its precursor  
494 compounds in aerosol aqueous-phase.

495 The size distribution of  $\omega C_2$  and Gly is similar to that of  $C_2$  diacid in the Okinawa samples  
496 (Figure 5e and f). The enrichment of  $\omega C_2$  and Gly in fine mode may be associated with enhanced  
497 secondary formation via aqueous-phase processing of their precursors during long-range transport.  
498 This interpretation is evidenced by the fact that strong correlations of  $\omega C_2$  and Gly were found with

499  $\text{SO}_4^{2-}$  ( $r = 0.96$  and  $0.86$ , respectively) and LWC ( $0.95$ ) in fine mode. The fine mode  $\omega\text{C}_2$  and Gly  
500 can also be produced primarily from biomass burning in East Asia and long-range transported to  
501 Okinawa. Significant positive correlations between  $\omega\text{C}_2$  and  $\text{K}^+$  ( $r = 0.90$ ), and Gly and  $\text{K}^+$  ( $0.86$ )  
502 suggest that biomass burning contributed significantly to the fine mode  $\omega\text{C}_2$  and Gly in Okinawa  
503 aerosols. Gly is a well-known precursor of  $\omega\text{C}_2$  and  $\text{C}_2$  in atmospheric aerosols (Lim et al., 2005;  
504 Ervens et al., 2010; Myriokefalitakis et al., 2011). The preferential enrichment of Gly and  $\omega\text{C}_2$  in  
505 fine mode can form  $\text{C}_2$  in Okinawa aerosols by aqueous-phase processing.

506 High correlations among  $\text{C}_2$ ,  $\omega\text{C}_2$  and Gly in fine mode ( $r = 0.92$ - $0.99$ ) also indicate their similar  
507 sources and formation processes and that  $\text{C}_2$  diacid may be produced by the oxidation of  $\omega\text{C}_2$  and  
508 Gly in fine mode. There is no significant difference in the slope of regression line of  $\text{C}_2$  with  $\omega\text{C}_2$   
509 between the fine and coarse modes (Figure S3g-h and Table S1) whereas the slope of regression  
510 line of  $\text{C}_2$  with Gly is significantly higher in fine mode than coarse mode (Figure S3i-j and Table  
511 S1). It is also remarkable that the slope of linear regression of  $\text{C}_2$  with Gly is significantly higher  
512 than that with  $\omega\text{C}_2$  in fine mode (Figure S3g-i and Table S2). This result may indicate a possible  
513 formation of fine mode oxalic acid from glyoxal via glyoxylic acid as an intermediate during long-  
514 range atmospheric transport in the western North Pacific.

515 The enrichment of  $\text{C}_2$ ,  $\omega\text{C}_2$  and Gly in fine mode in Okinawa was probably due to the enhanced  
516 oxidation of anthropogenic precursors emitted in East Asia during long-range transport because  
517 their size distributions are consistent with that of Ph and benzoic acid (Figure 5g and h), which are  
518 tracers of anthropogenic sources. The strong correlations of fine mode  $\text{C}_2$ ,  $\omega\text{C}_2$  and Gly with Ph ( $r =$   
519  $0.85$ - $0.93$ ) and benzoic acid ( $r = 0.90$ - $0.96$ ) further suggest that anthropogenic precursors are their  
520 important sources in fine mode. Ph and benzoic acid are directly emitted from combustion sources  
521 and secondarily produced in the atmosphere by the photooxidation of aromatic hydrocarbons  
522 emitted from the incomplete combustion of fossil fuel (Kawamura et al., 1985; Kawamura and  
523 Kaplan, 1987; Ho et al., 2006).

524 Aromatic hydrocarbons such as naphthalene and toluene have been suggested as major  
525 precursors of Ph and benzoic acid, respectively (Schauer et al., 1996; Kawamura and Yasui, 2005).  
526 Based on the high levels of naphthalene and toluene in China (Liu et al., 2007; Tao et al., 2007;

527 Duan et al., 2008), Ho et al. (2015) recently suggested that oxidation of naphthalene and toluene in  
528 the atmosphere is one of major source of Ph and benzoic acid, respectively. High levels of  
529 precursors in the source regions might favor the significant secondary production of Ph and benzoic  
530 acid during long-range transport in the western North Pacific. It may be possible that their  
531 precursors emitted in East Asia were taken up by aqueous-phase aerosol and oxidized to result in Ph  
532 and benzoic acid in fine mode during long-range transport. Moreover, enrichment of Ph and  
533 benzoic acid in fine mode further suggests that these species are associated with combustion  
534 sources either by primary emission and/or secondary production from the precursor compounds,  
535 being consistent with other anthropogenic  $\text{SO}_4^{2-}$ ,  $\text{NH}_4^+$  and  $\text{K}^+$ . Fine mode Ph can also be produced  
536 from evaporation of phthalates from plastics used in populated and industrialized regions in East  
537 Asia and long-range transported to Okinawa as discussed earlier. This explanation is consistent with  
538 the enrichment of terephthalic acid (tPh) in fine mode (Figure 5i), which is a tracer of plastic  
539 burning (Kawamura and Pavuluri, 2011).

#### 540 **3.4.2 C<sub>9</sub> and $\omega$ C<sub>9</sub>**

541 The second group of organic compounds, including C<sub>9</sub> and  $\omega$ C<sub>9</sub>, showed bimodal size distribution  
542 with a major peak on coarse mode at 3.3-4.7  $\mu\text{m}$  and minor peak on fine mode at 0.65-1.1  $\mu\text{m}$   
543 (Figure 5j and k). The strong correlations were found between C<sub>9</sub> and  $\text{Na}^+$  ( $r = 0.85$ ), and  $\omega$ C<sub>9</sub> and  
544  $\text{Na}^+$  (0.83) in coarse mode, indicating that C<sub>9</sub> and  $\omega$ C<sub>9</sub> may be emitted into the atmosphere from the  
545 sea surface microlayers together with sea salt particles in Okinawa. Kawamura and Gagosian  
546 (1987) suggested that C<sub>9</sub> and  $\omega$ C<sub>9</sub> are also derived from the photooxidation of unsaturated fatty  
547 acids such as oleic acid (C<sub>18:1</sub>) that are produced by phytoplankton and emitted from sea surface  
548 microlayers as sea salt particles. The laboratory experiments also documented the formation of C<sub>9</sub>  
549 and  $\omega$ C<sub>9</sub> due to photooxidation of C<sub>18:1</sub> (Matsunaga et al., 1999; Huang et al., 2005; Ziemann, 2005;  
550 Tedetti et al., 2007). Sea surface microlayers in the surroundings of Okinawa can also emit  
551 unsaturated fatty acids together with sea salts. Therefore, the major peaks of C<sub>9</sub> and  $\omega$ C<sub>9</sub> on the  
552 coarse mode may be derived from heterogeneous oxidation of unsaturated fatty acids of marine  
553 phytoplankton origin on the sea salt particles.

554 Wang et al. (2011) suggested that unsaturated fatty acids can be directly emitted as fine particles  
555 from food cooking emission in urban area in China and be oxidized to C<sub>9</sub> diacid in fine mode. The  
556 minor peak of C<sub>9</sub> and ωC<sub>9</sub> in fine mode can be explained by the oxidation of fine-mode unsaturated  
557 fatty acids derived from food cooking or gaseous unsaturated fatty acids during long-range transport  
558 to the western North Pacific.

### 559 3.5 Ratios of selected diacids

560 Kawamura and Ikushima (1993) proposed that malonic to succinic acid ratio (C<sub>3</sub>/C<sub>4</sub>) is a tracer to  
561 evaluate the extent of photochemical processing of organic aerosols. Because C<sub>4</sub> is oxidized to C<sub>3</sub>,  
562 an increase in the C<sub>3</sub>/C<sub>4</sub> ratio indicates an increased photochemical processing. The average C<sub>3</sub>/C<sub>4</sub>  
563 ratio in sum of all the size fractions was found to be 1.5±0.1 in Okinawa aerosols. This result  
564 suggests that the extent of photochemical processing is much greater in Okinawa than Los Angeles  
565 (0.35) (Kawamura and Kaplan, 1987) but similar to that of urban Tokyo (1.5) (Kawamura and  
566 Ikushima, 1993), whereas it is lower than those of marine aerosols at Chichijima Island in the  
567 western North Pacific (2.0) (Mochida et al., 2003b) and the remote Pacific including tropics (3.9)  
568 (Kawamura and Sakaguchi, 1999). Figure 8a shows changes in the C<sub>3</sub>/C<sub>4</sub> ratios as a function of  
569 particle size. The C<sub>3</sub>/C<sub>4</sub> ratios exhibit higher values at 1.1-2.1 μm in fine mode and at 2.1-3.3 and  
570 3.3-4.7 μm in coarse mode. This result suggests that C<sub>3</sub> production via C<sub>4</sub> decomposition occurs  
571 more efficiently at these size ranges by aqueous-phase processing.

572 Ph diacid originates from various anthropogenic sources whereas C<sub>9</sub> diacid is specifically  
573 produced by the oxidation of biogenic unsaturated fatty acids (Kawamura and Gagosian, 1987;  
574 Kawamura and Ikushima, 1993). Therefore, Ph/C<sub>9</sub> ratio is most likely used as a tracer to understand  
575 the source strength of anthropogenic v.s. biogenic sources of diacids. Higher Ph/C<sub>9</sub> ratio shows  
576 more influence of anthropogenic sources whereas lower ratio shows more influence of biogenic  
577 sources. Figure 8b presents changes in the ratios of Ph/C<sub>9</sub> as a function of particle sizes. The higher  
578 Ph/C<sub>9</sub> ratios were obtained on fine mode particles than coarse mode particles. These results suggest  
579 that fine aerosols in Okinawa are significantly influenced by anthropogenic sources whereas the  
580 coarse aerosols are more influenced by biogenic sources. A significant contribution of Ph on fine

581 mode further supports that anthropogenic sources are an important source of diacids and related  
582 compounds in fine mode of Okinawa aerosols.

#### 583 **4 Summary and conclusions**

584 Nine-stage atmospheric particles from  $<0.43$  to  $>11.3$   $\mu\text{m}$  in diameter, collected in spring 2008 at  
585 Cape Hedo, Okinawa in the western North Pacific Rim, were analyzed for water-soluble diacids  
586 and related compounds as well as water-soluble organic carbon (WSOC), organic carbon (OC) and  
587 inorganic ions. The molecular distributions of diacids were characterized by the predominance of  
588 oxalic acid ( $\text{C}_2$ ) followed by malonic ( $\text{C}_3$ ) and succinic ( $\text{C}_4$ ) acids in all stages, suggesting that they  
589 are most likely produced by the photooxidation of VOCs and particulate organic precursors in the  
590 source region and/or during long-range atmospheric transport. The abundant presence of  $\text{SO}_4^{2-}$  as  
591 well as phthalic and adipic acids in Cape Hedo suggested a significant contribution of  
592 anthropogenic sources including industrial emissions in East Asia to Okinawa aerosols via long-  
593 range atmospheric transport.

594  $\text{SO}_4^{2-}$ ,  $\text{NH}_4^+$ , and diacids up to 5-carbon atoms as well as glyoxylic acid ( $\omega\text{C}_2$ ) and glyoxal (Gly)  
595 showed good correlations with peaks in fine mode (0.65-1.1  $\mu\text{m}$ ). WSOC and OC also peaked on  
596 fine mode with an additional minor peak on coarse mode. Similar size distributions and strong  
597 correlations of diacids ( $\text{C}_2$ - $\text{C}_5$ ),  $\omega\text{C}_2$  and Gly with  $\text{SO}_4^{2-}$  in fine mode suggest their secondary  
598 formation possibly in aerosol aqueous-phase. Their strong correlations with LWC in fine mode  
599 further suggest an importance of the aqueous-phase production in Okinawa aerosols. They may  
600 have also been directly emitted from biomass burning as supported by strong correlations with  $\text{K}^+$   
601 in fine mode. The robust correlations of  $\text{C}_2$  with  $\text{C}_3$ - $\text{C}_5$  diacids as well as  $\omega\text{C}_2$  and Gly indicate that  
602 they are the key precursors of  $\text{C}_2$  diacid in Okinawa aerosols.

603 Longer-chain diacid ( $\text{C}_9$ ) and  $\omega$ -oxoacid ( $\omega\text{C}_9$ ) showed bimodal size distribution with a major  
604 peak on coarse mode, suggesting that they were directly emitted and/or produced by photooxidation  
605 of unsaturated fatty acids mainly derived from sea surface microlayers via heterogeneous reactions  
606 on sea spray particles. We observed that WSOC and OC in fine particles are photochemically more  
607 processed in the atmosphere than in coarse particles during long-range transport. This study

608 demonstrates that anthropogenic and biomass burning aerosols emitted from East Asia have  
609 significant influence on the molecular compositions of water-soluble organic aerosols in the  
610 western North Pacific Rim.

### 611 **Acknowledgement**

612 We acknowledge the financial support from the Japan Society for the Promotion of Science (JSPS)  
613 through Grant-in-Aid Nos. 1920405 and 24221001. We appreciate the financial support of the JSPS  
614 fellowship to D. K. Deshmukh. We also acknowledge the support of ENSCR to M. Lazaar for the  
615 summer student program in Japan. The authors gratefully appreciate the NOAA Air Resources  
616 Laboratory (ARL) for the provision of the HYSPLIT transport and dispersion model  
617 (<http://www.ready.noaa.gov>) for seven-day air mass backward trajectories of sampling site Cape  
618 Hedo for each sampling period. We thank E. Tachibana for the analyses of OKI-5 samples and M.  
619 Mochida, S. Aggarwal and Y. Kitamori for the helps during the campaign. The authors appreciate  
620 the critical and useful comments by anonymous reviewers, which significantly improved the quality  
621 of manuscript.

622

623 **References**

- 624 Ansari, A. S. and Pandis, S. N.: Water absorption by secondary organic aerosol and its effect on  
625 inorganic aerosol behavior, *Environ. Sci. Technol.*, 34, 71-77, 2000.
- 626 Agarwal, S., Aggarwal, S. G., Okuzawa, K., and Kawamura, K.: Size distributions of dicarboxylic  
627 acids, ketoacids, alpha-dicarbonyls, sugars, WSOC, OC, EC and inorganic ions in  
628 atmospheric particles over Northern Japan: implication for long-range transport of Siberian  
629 biomass burning and East Asian polluted aerosols, *Atmos. Chem. Phys.*, 10, 5839-5858,  
630 2010.
- 631 Aggarwal, S. G. and Kawamura, K.: Carbonaceous and inorganic composition in long-range  
632 transported aerosols over northern Japan: implications for aging of water-soluble organic  
633 fraction, *Atmos. Environ.*, 43, 2532-2540, 2009.
- 634 Andreas, E.L.: A new sea spray generation function for wind speeds up to  $32 \text{ m s}^{-1}$ , *J. Phys.*  
635 *Oceanogr.*, 28, 2175-2184, 1998.
- 636 Bian, Q., Huang, X. H. H., and Yu, J. Z.: One-year observations of size distribution characteristics  
637 of major aerosol constituents at a coastal site in Hong Kong - Part 1: Inorganic ions and  
638 oxalate, *Atmos. Chem. Phys.*, 14, 9013-9027, 2014.
- 639 Boreddy, S. K. R. and Kawamura K.: A 12-year observation of water-soluble inorganic ions in TSP  
640 aerosols collected at a remote marine location in the western North Pacific: An outflow region  
641 of Asian dust, *Atmos. Chem. Phys.*, 15, 6437-6453, 2015.
- 642 Carlton, A. G., Turpin, B. J., Altieri, K. E., Seitzinger, S., Reff, A., Lim, H. J., and Ervens, B.:  
643 Atmospheric oxalic acid and SOA production from glyoxal: Results of aqueous  
644 photooxidation experiments, *Atmos. Environ.*, 41, 7588-7602, 2007.
- 645 Carlton, A. G., Turpin, B. J., Lim, H. J., Altieri, K. E., and Seitzinger, S.: Link between isoprene  
646 and secondary organic aerosol (SOA): Pyruvic acid oxidation yields low volatility organic  
647 acids in clouds, *Geophys. Res. Lett.*, 33, L06822, doi:10.1029/2005GL025374, 2006.
- 648 Davidson, C. I., Phalen, R. F., and Solomon, P. A.: Airborne particulate matter and human health: A  
649 review, *Aerosol. Sci. Tech.*, 39, 737-749, 2005.
- 650 Draxler, R. R. and Rolph, G. D.: HYSPLIT (HYbrid Single-Particle Lagrangian Integrated Trajec-  
651 tory) Model, available at: <http://www.arl.noaa.gov/HYSPLIT.php> (last access: 5 January  
652 2015), NOAA Air Resources Laboratory, College Park, MD.
- 653 Duan, J. C., Tan, J. H., Yang, L., Wu, S., and Hao, J. M.: Concentration, sources and ozone  
654 formation potential of volatile organic compounds (VOCs) during ozone episode in Beijing,  
655 *Atmos. Res.*, 88, 25-35, 2008.
- 656 Engelhart, G. J., Hildebrandt, L., Kostenidou, E., Mihalopoulos, N., Donahue, N. M., and Pandis, S.  
657 N.: Water content of aged aerosol, *Atmos. Chem. Phys.*, 11, 911-920, 2011.
- 658 Engling, G., Lee, J. J., Sie, H. J., Wu, Y. C., and Yet-Pole, I.: Anhydrosugar characteristics in  
659 biomass smoke aerosol-case study of environmental influence on particle-size of rice straw  
660 burning aerosol, *J. Aerosol Sci.*, 56, 2-14, 2013.
- 661 Irei, S., Takami, A., Hayashi, M., Sadanaga, Y., Hara, K., Kaneyasu, N., Sato, K., Arakaki, T.,  
662 Hatakeyama, S., Bandow, H., Hikida, T., and Shimono, A.: Transboundary secondary organic

- 663 aerosol in western Japan indicated by the  $\delta^{13}\text{C}$  of water-soluble organic carbon and the  $m/z$  44  
664 signal in organic aerosol mass spectra, *Environ. Sci. Technol.*, 48, 6273-6281, 2014.
- 665 Ervens, B., Carlton, A. G., Turpin, B. J., Altieri, K. E., Kreidenweis, S. M., and Feingold, G.:  
666 Secondary organic aerosol yields from cloud-processing of isoprene oxidation products,  
667 *Geophys. Res. Lett.*, 35, L02816, doi:10.1029/2007gl031828, 2008.
- 668 Ervens, B., Cubison, M., Andrews, E., Feingold, G., Ogren, J. A., Jimenez, J. L., DeCarlo, P., and  
669 Nenes, A.: Prediction of cloud condensation nucleus number concentration using  
670 measurements of aerosol size distributions and composition and light scattering enhancement  
671 due to humidity, *J. Geophys. Res.*, 112, D10S32, doi:10.1029/2006jd007426, 2007.
- 672 Ervens, B. and Volkamer, R.: Glyoxal processing by aerosol multiphase chemistry: towards a  
673 kinetic modeling framework of secondary organic aerosol formation in aqueous particles,  
674 *Atmos. Chem. Phys.*, 10, 8219-8244, 2010.
- 675 Falkovich, A. H., Graber, E. R., Schkolnik, G., Rudich, Y., Maenhaut, W., and Artaxo, P.: Low  
676 molecular weight organic acids in aerosol particles from Rondonia, Brazil, during the  
677 biomass-burning, transition and wet periods, *Atmos. Chem. Phys.*, 5, 781-797, 2005.
- 678 Fountoukis, C. and Nenes, A.: ISORROPIA II: a computationally efficient thermodynamic  
679 equilibrium model for  $\text{K}^+$ - $\text{Ca}^{2+}$ - $\text{Mg}^{2+}$ - $\text{NH}_4^+$ - $\text{Na}^+$ - $\text{SO}_4^{2-}$ - $\text{NO}_3^-$ - $\text{Cl}^-$ - $\text{H}_2\text{O}$  aerosols, *Atmos. Chem.*  
680 *Phys.*, 7, 4639-4659, 2007.
- 681 Gao, Y., Arimoto, R., Duce, R. A., Chen, L. Q., Zhou, M. Y., and Gu, D. Y.: Atmospheric non-sea-  
682 salt sulfate, nitrate and methanesulfonate over the China Sea, *J. Geophys. Res.*, 101, 12601-  
683 12611, 1996.
- 684 Gao, X., Xue, L., Wang, X., Wang, T., Yuan, T., Gao, R., Zhou, Y., Nie, W., Zhang, Q., and Wang,  
685 W.: Aerosol ionic components at Mt. Heng in central southern China: abundances, size  
686 distribution, and impacts of long-range transport, *Sci. Total Environ.*, 433, 498-506, 2012.
- 687 Geng, H., Park, Y., Hwang, H., Kang, S., and Ro, C. U.: Elevated nitrogen-containing particles  
688 observed in Asian dust aerosol samples collected at the marine boundary layer of the Bohai  
689 Sea and the Yellow Sea, *Atmos. Chem. Phys.*, 9, 6933-6947, 2009.
- 690 Geng, C. and Mu, Y.: Carbonyl sulfide and dimethyl sulfide exchange between trees and the  
691 atmosphere, *Atmos. Environ.*, 40, 1373-1383, 2006.
- 692 Hagler, G. S. W., Bergin, M. H., Smith, E. A., and Dibb, J. E.: A summer time series of particulate  
693 carbon in the air and snow at Summit, Greenland, *J. Geophys. Res.*, 112, D21309,  
694 doi:10.1029/2007JD008993, 2007.
- 695 Hanisch, F. and Crowley, J.N.: Heterogeneous reactivity of gaseous nitric acid on  $\text{Al}_2\text{O}_3$ ,  $\text{CaCO}_3$ ,  
696 and atmospheric dust samples: A Knudsen cell study, *J. Phys.Chem. (A)*, 105, 3096-3106,  
697 2001a.
- 698 Hanisch, F. and Crowley, J.N.: The heterogeneous reactivity of gaseous nitric acid on authentic  
699 mineral dust samples, and on individual mineral and clay mineral components, *Phys. Chem.*  
700 *Chem. Phys.*, 3, 2474-2482, 2001b.
- 701 Hatakeyama, S., Tanonaka, T., Weng, J., Bandow, H., Takagi, H., and Akimoto, H.: Ozone-  
702 cyclohexene reaction in air: quantitative analyses of particulate products and the reaction  
703 mechanism, *Environ. Sci. Technol.*, 19, 935-942, 1985.



- 704 Ho, K. F., Lee, S. C., Cao, J. J., Kawamura, K., Watanabe, T., Cheng, Y., and Chow, J. C.:  
705 Dicarboxylic acids, ketocarboxylic acids and dicarbonyls in the urban roadside area of Hong  
706 Kong, *Atmos. Environ.*, 40, 3030-3040, 2006.
- 707 Ho, K. F., Huang, R. -J., Kawamura, K., Tachibana, E., Lee, S. C., Ho, S. S. H., Zhu, T., and Tian,  
708 L.: Dicarboxylic acids, ketocarboxylic acids,  $\alpha$ -dicarbonyls, fatty acids and benzoic acid in  
709 PM<sub>2.5</sub> aerosol collected during CAREBeijing-2007: an effect of traffic restriction on air  
710 quality, *Atmos. Chem. Phys.*, 15, 3111-3123, 2015.
- 711 Huang, H. -M., Katrib, Y., and Martin, S. C.: Products and mechanisms of the reaction of oleic acid  
712 with ozone and nitrate radical, *J. Phys. Chem. A*, 109, 4517-4530, 2005.
- 713 Huang, X. F., Yu, J. Z., He, L. Y., and Yuan, Z. B.: Water-soluble organic carbon and oxalate in  
714 aerosols at a coastal urban site in China: Size distribution characteristics, sources, and  
715 formation mechanisms, *J. Geophys. Res.*, 111, D22212, doi:10.1029/2006JD007408, 2006.
- 716 Jacobson, M. Z.: *Atmospheric Pollution: History, Science, and Regulation*. Cambridge University  
717 Press, United Kingdom, 2002.
- 718 Jacobson, M. C., Hansson, H. C., Noone, K. J., and Charlson, R. J.: Organic atmospheric aerosols:  
719 Review and state of science, *Rev. Geophys.*, 38, 267-294, 2000.
- 720 Jafferson, A., Tanner, D. J., Eisele, F. L., Davis, D. D., Chen, G., Creawford, J., Huey, J. W.,  
721 Torres, A. L., and Berresheim, H.: OH photochemistry and methane sulfonic acid formation  
722 in the coastal Antarctic boundary layer, *J. Geophys. Res.*, 103, 1647-1656, 1998.
- 723 Kalberer, M., Yu, J., Cocker, D. R., Flagan, R. C., and Seinfeld, J. H.: Aerosol formation in the  
724 cyclohexene-ozone system, *Environ. Sci. Technol.*, 34, 4894- 4901, 2000.
- 725 Kanakidou, M., Seinfeld, J. H., Pandis, S. N., Barnes, I., Dentener, F. J., Facchini, M. C., Van  
726 Dingenen, R., Ervens, B., Nenes, A., Nielsen, C. J., Swietlicki, E., Putaud, J. P., Balkanski,  
727 Y., Fuzzi, S., Horth, J., Moortgat, G. K., Winterhalter, R., Myhre, C. E. L., Tsigaridis, K.,  
728 Vignati, E., Stephanou, E. G., and Wilson, J.: Organic aerosol and global climate modelling: a  
729 review, *Atmos. Chem. Phys.*, 5, 1053-1123, 2005.
- 730 Kaufman, Y. J. and Fraser, R. S.: The effect of smoke particles on clouds and climate forcing,  
731 *Science*, 277, 1636-1639, 1997.
- 732 Kawamura, K. and Gagosian, R. B.: Implications of  $\omega$ -oxocarboxylic acids in the remote marine  
733 atmosphere for photo-oxidation of unsaturated fatty acids, *Nature*, 325, 330-332, 1987.
- 734 Kawamura, K. and Ikushima, K.: Seasonal changes in the distribution of dicarboxylic acids in the  
735 urban atmosphere, *Environ. Sci. Technol.*, 27, 2227-2235, 1993.
- 736 Kawamura, K. and Kaplan, I. R.: Motor Exhaust Emissions as a Primary Source for Dicarboxylic-  
737 Acids in Los-Angeles Ambient Air, *Environ. Sci. Technol.*, 21, 105-110, 1987.
- 738 Kawamura, K. and Sakaguchi, F.: Molecular distributions of water soluble dicarboxylic acids in  
739 marine aerosols over the Pacific Ocean including tropics, *J. Geophys. Res.*, 104, 3501-3509,  
740 1999.
- 741 Kawamura, K. and Usukura, K.: Distributions of low molecular weight dicarboxylic acids in the  
742 North Pacific aerosol samples, *J. Oceanogr.*, 49, 271-283, 1993.

- 743 Kawamura, K., Imai, Y., and Barrie, L. A.: Photochemical production and loss of organic acids in  
744 high Arctic aerosols during long-range transport and polar sunrise ozone depletion events,  
745 *Atmos. Environ.*, 39, 599-614, 2005.
- 746 Kawamura, K., Kasukabe, H., and Barrie, L. A.: Source and reaction pathways of dicarboxylic  
747 acids, ketoacids and dicarbonyls in arctic aerosols: One year of observations, *Atmos.*  
748 *Environ.*, 30, 1709-1722, 1996.
- 749 Kawamura, K., Narukawa, M., Li, S. M., and Barrie, L. A.: Size distributions of dicarboxylic acids  
750 and inorganic ions in atmospheric aerosols collected during polar sunrise in the Canadian high  
751 Arctic, *J. Geophys. Res.*, 112, D10307, doi:10.1029/2006JD008244, 2007.
- 752 Kawamura, K., Ng, L., and Kaplan, I. R., Determination of organic acids (C<sub>1</sub>-C<sub>10</sub>) in the  
753 atmosphere, motor-exhausts and engine oils, *Environ. Sci. Technol.*, 19, 1082-1086, 1985.
- 754 Kawamura, K. and Pavuluri, C.M.: New Directions: Need for better understanding of plastic waste  
755 burning as inferred from high abundance of terephthalic acid in South Asian aerosols, *Atmos.*  
756 *Environ.*, 44, 5320-5321, 2011.
- 757 Kawamura, K. and Yasui, O.: Diurnal changes in the distribution of dicarboxylic acids,  
758 ketocarboxylic acids and dicarbonyls in the urban Tokyo atmosphere, *Atmos. Environ.*, 39,  
759 1945-1960, 2005.
- 760 Kawamura, K. and Bikkina, S.: A review of dicarboxylic acids and related compounds in  
761 atmospheric aerosols: Molecular distributions, sources and transformation, *Atmos. Res.*, 170,  
762 140-160, 2016.
- 763 Kawamura, K.: Identification of C<sub>2</sub>-C<sub>10</sub> ω-oxocarboxylic acids, pyruvic acid, and C<sub>2</sub>-C<sub>3</sub> α-  
764 dicarbonyls in wet precipitation and aerosol samples by capillary GC and GC/MS, *Anal.*  
765 *Chem.*, 65, 3505-3511, 1993.
- 766 Kerminen, V. -M., Pakkanen, T. A., and Hillamo, R. E.: Interactions between inorganic trace gases  
767 and supermicrometer particles at a coastal site, *Atmos. Environ.*, 31, 2753-2765, 1997a.
- 768 Kerminen, V. -M., Aurela, M., Hillamo, R. E., and Virkkula, A.: Formation of particulate MSA:  
769 deductions from size distribution measurements in the Finnish Arctic, *Tellus*, 49b, 159-171,  
770 1997b.
- 771 Kleeman, M. J. and Cass, G. R.: Effect of emissions control strategies on the size and composition  
772 distribution of urban particulate air pollution, *Environ. Sci. Technol.*, 33, 177-189, 1999.
- 773 Kouyoumdjian, H. and Saliba, N. A.: Mass concentration and ion composition of coarse and fine  
774 particles in an urban area in Beirut: effect of calcium carbonate on the absorption of nitric and  
775 sulfuric acids and the depletion of chloride, *Atmos. Chem. Phys.*, 6, 1865-1877, 2006.
- 776 Kumar, A., Sarin, M. M., and Sudheer, A. K.: Mineral and anthropogenic aerosols in Arabian Sea-  
777 atmospheric boundary layer: Sources and spatial variability, *Atmos. Environ.*, 42, 5169-5181,  
778 2008.
- 779 Kundu S., Kawamura, K., Andreae, T. W., Hoffer, A., and Andreae, M. O.: Molecular distributions  
780 of dicarboxylic acids, ketocarboxylic acids and α-dicarbonyls in biomass burning aerosols:  
781 implications for photochemical production and degradation in smoke layers, *Atmos. Chem.*  
782 *Phys.*, 10, 2209-2225, 2010.

- 783 Kunwar, B. and Kawamura, K.: Seasonal distribution and sources of low molecular weight  
784 dicarboxylic acids,  $\omega$ -oxocarboxylic acids, pyruvic acid,  $\alpha$ -dicarbonyls and fatty acids in  
785 ambient aerosols from subtropical Okinawa in the western Pacific Rim, *Environ. Chem.*, 11,  
786 673-689, 2014.
- 787 Legrand, M., Preunkert, S., Oliveira, T., Pio, C. A., Hammer, S., Gelencser, A., Kasper-Giebl, A.,  
788 and Laj, P.: Origin of C<sub>2</sub>-C<sub>5</sub> dicarboxylic acids in the European atmosphere inferred from  
789 year-round aerosol study conducted at a west-east transect, *J. Geophys. Res.*, 112, D23S07,  
790 doi:10.1029/2006JD008019, 2007.
- 791 Lim, H. J., Carlton, A. G., and Turpin, B. J.: Isoprene forms secondary organic aerosol through  
792 cloud processing: Model simulations, *Environ. Sci. Technol.*, 39, 4441-4446, 2005.
- 793 Lim, Y. B., Tan, Y., Perri, M. J., Seitzinger, S. P., and Turpin, B. J.: Aqueous chemistry and its role  
794 in secondary organic aerosol (SOA) formation, *Atmos. Chem. Phys.*, 10, 10521-10539, 2010.
- 795 Liu, S. Z., Tao, S., Liu, W. X., Liu, Y. N., Dou, H., Zhao, J. Y., Wang, L. G., Wang, J. F., Tian, Z.  
796 F., and Gao, Y.: Atmospheric polycyclic aromatic hydrocarbons in north China: A winter-  
797 time study, *Environ. Sci. Technol.*, 41, 8256-8261, 2007.
- 798 Matsunaga, S., Kawamura, K., Nakatsuka, T., and Ohkouchi, N.: Preliminary study on laboratory  
799 photochemical formation of low molecular weight dicarboxylic acids from unsaturated fatty  
800 acid (oleic acid), *Res. Org. Geochem.*, 14, 19-25, 1999.
- 801 Mayol-Bracero, O. L., Guyon, P., Graham, B., Roberts, G., Andreae, M. O., Decesari, S., Facchini,  
802 M. C., Fuzzi, S., and Artaxo, P.: Water-soluble organic compounds in biomass burning  
803 aerosols over Amazonia - 2. Apportionment of the chemical composition and importance of  
804 the polyacidic fraction, *J. Geophys. Res.*, 107, 8091, doi:10.1029/2001jd000522, 2002.
- 805 Meinardi, S., Simpson, I. J., Blake, N. J., Blake, D. R., and Rowland, E. S.: Dimethyl disulfide  
806 (DMDS) and dimethyl sulfide (DMS) emissions from biomass burning in Australia, *Geophys.*  
807 *Res. Lett.*, 30, 1454, doi:10.1029/2003GL016967, 2003.
- 808 Mkoma, S. L., Kawamura, K., and Fu, P. Q.: Contributions of biomass/biofuel burning to organic  
809 aerosols and particulate matter in Tanzania, East Africa, based on analyses of ionic species,  
810 organic and elemental carbon, levoglucosan and mannosan, *Atmos. Chem. Phys.*, 13, 10325-  
811 10338, 2013.
- 812 Miyazaki, Y., Kawamura, K., and Sawano, M.: Size distributions and chemical characterization of  
813 water-soluble organic aerosols over the western North Pacific in summer, *J. Geophys. Res.*,  
814 115, D23210, doi:10.1029/2010JD014439, 2010.
- 815 Miyazaki, Y., Kawamura, K., Jung, J., Furutani, H., and Uematsu, M.: Latitudinal distributions of  
816 organic nitrogen and organic carbon in marine aerosols over the western North Pacific,  
817 *Atmos. Chem. Phys.*, 11, 3037-3049, 2011.
- 818 Mochida, M., Kawabata, A., Kawamura, K., Hatsushika, H., and Yamazaki, K.: Seasonal variation  
819 and origins of dicarboxylic acids in marine atmosphere over the western North Pacific, *J.*  
820 *Geophys. Res.*, 108, 4193, doi:10.1029/2002JD002355, 2003b.
- 821 Mochida, M., Umemoto, N., Kawamura, K., and Uematsu, M.: Bimodal size distribution of C<sub>2</sub>-C<sub>4</sub>  
822 dicarboxylic acids in the marine aerosols, *Geophys. Res. Lett.*, 30, 1672, doi:  
823 10.1029/2003GL017451, 2003a.

- 824 Mochida, M., Umemoto, N., Kawamura, K., Lim, H. J., and Turpin, B. J.: Bimodal size  
825 distributions of various organic acids and fatty acids in the marine atmosphere: Influence of  
826 anthropogenic aerosols, Asian dusts, and sea spray off the coast of East Asia, *J. Geophys.*  
827 *Res.*, 112, D15209, doi:10.1029/2006JD007773, 2007.
- 828 Myriokefalitakis, S., Tsigaridis, K., Mihalopoulos, N., Sciare, J., Nenes, A., Kawamura, K., Segers,  
829 A., and Kanakidou, M.: In-cloud oxalae formation in the regional troposphere: a 3-D  
830 modelling study, *Atmos. Chem. Phys.*, 11, 5761-5782, 2011.
- 831 Nenes, A., Pandis, S. N., and Pilinis, C.: ISORROPIA: A new thermodynamic equilibrium model  
832 for multiphase multicomponent inorganic aerosols, *Aquat. Geochem.*, 4, 123-152, 1998.
- 833 Pakkanen, T. A., Loukkola, K., Korhonen, C. H., Aurela, M., Makela, T., Hillamo, R. E., Aarnio,  
834 P., Koskentalo, T., Kousa, A., and Maenhaut, W.: Sources and chemical composition of  
835 atmospheric fine and coarse particles in the Helsinki area, *Atmos. Environ.*, 35, 5381-5391,  
836 2001.
- 837 Pavuluri, C. M., Kawamura, K., Mihalopoulos, N., and Swaminathan, T.: Laboratory  
838 photochemical processing of aqueous aerosols: formaion and degradation of dicarboxylic  
839 acids, oxocarboxylic acids, and alpha-dicarbonyls, *Atmos. Chem. Phys.*, 15, 7999-8012, 2015.
- 840 Pope, C. A. and Dockery, D. W.: Health effects of fine particulate air pollution: Lines that connect,  
841 *J. Air Waste Manage.*, 56, 709-742, 2006.
- 842 Pradeep Kumar, P., Broekhuizen, K., and Abbatt, J. P. D.: Organic acids as cloud condensation  
843 nuclei: Laboratory studies of highly soluble and insoluble species, *Atmos. Chem. Phys.*, 3,  
844 509-520, 2003.
- 845 Quinn, P. K., Covert, D. S., Bates, T. S., Kapustin, V. N., Ramseybell, D. C., and Mcinnes, L. M.:  
846 Dimethylsulfide cloud condensation nuclei climate system - relevant size-resolved  
847 measurements of the chemical and physical-properties of atmospheric aerosol-particles, *J.*  
848 *Geophys. Res.*, 98, 10411-10427, 1993.
- 849 Ramanathan, V., Crutzen, P. J., Kiehl, J. T., and Rosenfeld, D.: Atmosphere - Aerosols, climate,  
850 and the hydrological cycle, *Science*, 294, 2119-2124, 2001.
- 851 Schauer, J. J., Rogge, W. F., Hildemann, L. M., Mazurek, M. A., and Cass, G. R.: Source  
852 apportionment of airborne particualte matter using organic compounds as tracers, *Atmos.*  
853 *Environ.*, 30, 3837-3855, 1996.
- 854 Seinfeld, J. H. and Pandis, S. N.: Atmospheric chemistry and physics: From air pollution to climate  
855 change, 2<sup>nd</sup> edition, J. Wiley, New York, 2006.
- 856 Seinfeld, J. H. and Pandis, S. N.: Atmospheric Chemistry and Physics, John Wiley & Sons, New  
857 York, 1998.
- 858 Seinfeld, J. H. and Pankow, J. F.: Organic atmospheric particulate material, *Annu. Rev. Phys.*  
859 *Chem.*, 54, 121-140, 2003.
- 860 Sempéré, R. and Kawamura, K.: Trans-hemispheric contribution of C<sub>2</sub>-C<sub>10</sub>  $\alpha,\omega$ -dicarboxylic acids,  
861 and related polar compounds to water-soluble organic carbon in the western Pacific aerosols  
862 in relation to photochemical oxidation reactions, *Glob. Biogeochem. Cycle*, 17, 1069,  
863 doi:10.1029/2002GB001980, 2003.

- 864 Shimada, K., Shimida, M., Takami, A., Hasegawa, S., Akihiro, F., Arakaki, T., Izumi, W., and  
865 Hatakeyama, S.: Mode and place of origin of carbonaceous aerosols transported from East  
866 Asia to Cape Hedo, Okinawa, Japan, *Aerosol Air. Qual. Res.*, 15, 799-813, 2015.
- 867 Simoneit, B. R. T., Medeiros, P. M., and Didyk, B. M.: Combustion products of plastics as  
868 indicators for refuse burning in the atmosphere, *Environ. Sci. Technol.*, 39, 6961-6970, 2005.
- 869 Speer, R. E., Edney, E. O., and Kleindienst, T. E.: Impact of organic compounds on the  
870 concentrations of liquid water in ambient PM<sub>2.5</sub>, *J. Aerosol Sci.*, 34, 63-77, 2003.
- 871 Takami, A., Miyoshi, T., Shimono, A., Kaneyasu, N., Kato, S., Kajii, Y., and Hatakeyama, S.:  
872 Transport of anthropogenic aerosols from Asia and subsequent chemical transformation, *J.*  
873 *Geophys. Res.*, 112, D22S31, doi 10.1029/2006jd008120, 2007.
- 874 Takiguchi, Y., Takami, A., Sadanaga, Y., Lun, X. X., Shimizu, A., Matsui, I., Sugimoto, N., Wang,  
875 W., Bandow, H., and Hatakeyama, S.: Transport and transformation of total reactive nitrogen  
876 over the East China Sea, *J. Geophys. Res.*, 113, D10306, doi:10.1029/2007jd009462, 2008.
- 877 Tao, J., Zhang, L., Engling, G., Zhang, R., Yang, T., Cao, J., Zhu, C., Wang, Q., and Luo, L.:  
878 Chemical composition of PM<sub>2.5</sub> in an urban environment in Chengdu, China: Importance of  
879 springtime dust storms and biomass burning, *Atmos. Res.*, 122, 270-283, 2013.
- 880 Tao, S., Wang, Y., Wu, S. M., Liu, S. Z., Dou, H., Liu, Y. N., Lang, C., Hu, F., and Xing, B. S.:  
881 Vertical distribution of polycyclic aromatic hydrocarbons in atmospheric boundary layer of  
882 Beijing in winter, *Atmos. Environ.*, 41, 9594-9602, 2007.
- 883 Tedetti, M., Kawamura, K., Narukawa, M., Joux, F., Charriere, B., and Sempéré, R.: Hydroxyl  
884 radical-induced photochemical formation of dicarboxylic acids from unsaturated fatty acid  
885 (oleic acid) in aqueous solution, *J. Photochem. Photobiol A.*, 188, 135-139, 2007.
- 886 Tsai, Y. I. and Chen, C. L.: Characterization of Asian dust storm and non-Asian dust storm PM<sub>2.5</sub>  
887 aerosol in southern Taiwan, *Atmos. Environ.*, 40, 4734-4750, 2006.
- 888 Turpin, B. J. and Lim, H. J.: Species contributions to PM<sub>2.5</sub> mass concentrations: Revisiting  
889 common assumptions for estimating organic mass, *Aerosol. Sci. Tech.*, 35, 602-610, 2001.
- 890 Volkamer, R., Platt, U., and Wirtz, K.: Primary and secondary glyoxal formation from aromatics:  
891 Experimental evidence for the bicycloalkyl-radical pathway from benzene, toluene, and p-  
892 xylene, *J. Phys. Chem. A*, 105, 7865-7874, 2001.
- 893 Wang, G. H., Kawamura, K., Xie, M. J., Hu, S. Y., Li, J. J., Zhou, B. H., Cao, J. J., and An, Z. S.:  
894 Selected water-soluble organic compounds found in size-resolved aerosols collected from  
895 urban, mountain and marine atmospheres over East Asia, *Tellus*, 63, 371-381, 2011.
- 896 Wang, G. H., Zhao, B. H., Cheng, C. L., Cao, J. J., Li, J. J., Meng, J. J., Tao, J., Zhang, R. J., and  
897 Fu, P. Q.: Impact of Gobi desert dust on aerosol chemistry of Xi'an, inland China during  
898 spring 2009: differences in composition and size distribution between the urban ground  
899 surface and the mountain atmosphere, *Atmos. Chem. Phys.*, 13, 819-835, 2013.
- 900 Wang, H., Kawamura, K., and Shooter, D.: Carbonaceous and ionic components in wintertime  
901 atmospheric aerosols from two New Zealand cities: Implication for solid fuel combustion,  
902 *Atmos. Environ.*, 39, 5865-5875, 2005a.

- 903 Wang, Y., Zhuang, G. S., Sun, Y., and An, Z. S.: Water-soluble part of the aerosol in the dust storm  
904 season - evidence of the mixing between mineral and pollution aerosols, *Atmos. Environ.*, 39,  
905 7020-7029, 2005b.
- 906 Warneck, P.: In-cloud chemistry opens pathway to the formation of oxalic acid in the marine  
907 atmosphere, *Atmos. Environ.*, 37, 2423-2427, 2003.
- 908 Yamasoe, M. A., Artaxo, P., Miguel, A. H., and Allen, A. G.: Chemical composition of aerosol  
909 particles from direct emissions of vegetation fires in the Amazon Basin: water-soluble species  
910 and trace elements, *Atmos. Environ.*, 34, 1641-1653, 2000.
- 911 Ziemann, P. J.: Aerosol products, mechanisms, and kinetics of heterogeneous reactions with oleic  
912 acid in pure and mixed particles, *Faraday Discuss.*, 130, 469-490, 2005.
- 913 Zimmermann, J. and Poppe, D.: A supplement for the RADM2 chemical mechanism: The  
914 photooxidation of isoprene, *Atmos. Environ.*, 30, 1255-1269, 1996.

**Table 1.** Concentrations ( $\mu\text{g m}^{-3}$ ) of major inorganic ions and carbonaceous species in the fine and coarse mode aerosols in Okinawa Island in the Western North Pacific.

Inorganic ions	Fine mode <sup>a</sup>				Coarse mode <sup>b</sup>			
	Mean	S.D. <sup>c</sup>	Min. <sup>d</sup>	Max. <sup>e</sup>	Mean	S.D.	Min.	Max.
Water-soluble inorganic ions								
Cations								
Na <sup>+</sup>	0.44	0.20	0.21	0.72	2.42	0.89	1.60	3.65
NH <sub>4</sub> <sup>+</sup>	2.40	1.18	0.74	3.69	0.03	0.01	0.03	0.05
K <sup>+</sup>	0.14	0.06	0.04	0.21	0.09	0.02	0.07	0.12
Mg <sup>2+</sup>	0.07	0.02	0.04	0.10	0.34	0.11	0.24	0.49
Ca <sup>2+</sup>	0.06	0.02	0.04	0.09	0.41	0.19	0.15	0.60
Total cations	3.12	1.22	1.28	4.37	3.29	1.02	2.55	4.82
Anions								
MSA <sup>-</sup>	0.04	0.01	0.03	0.06	0.01	0.00	0.00	0.01
Cl <sup>-</sup>	0.12	0.13	0.02	0.29	4.27	2.25	1.77	7.25
NO <sub>3</sub> <sup>-</sup>	0.14	0.08	0.04	0.23	1.61	0.54	0.94	2.41
SO <sub>4</sub> <sup>2-</sup>	10.1	4.85	2.88	14.9	1.46	0.44	0.69	1.81
Total anions	10.4	4.73	3.33	15.1	7.35	2.20	5.69	10.6
Total water-soluble ions								
Total water-soluble ions	13.5	5.95	4.61	19.5	10.6	3.22	8.33	15.4
Carbonaceous components								
WSOC	1.12	0.49	0.31	1.61	0.33	0.13	0.15	0.52
OC	1.62	0.59	0.62	2.12	0.60	0.17	0.36	0.82
OM	3.43	1.31	1.30	4.87	1.25	0.36	0.75	1.73
EC	0.05	0.03	0.00	0.09	-	-	-	-
TC	1.67	0.65	0.62	2.41	0.60	0.17	0.36	0.82

<sup>a</sup>Fine mode represents aerosol size of  $D_p < 2.1 \mu\text{m}$ .<sup>b</sup>Coarse mode represents aerosol size of  $D_p > 2.1 \mu\text{m}$ .<sup>c</sup>Standard deviation.<sup>d</sup>Minimum.<sup>e</sup>Maximum.

**Table 2.** Summarized concentrations (ng m<sup>-3</sup>) of water-soluble dicarboxylic acids and related polar compounds in the fine and coarse mode aerosols from Okinawa Island in the western North Pacific Rim.

Compounds	Abbreviation	Chemical formula	Fine mode <sup>a</sup>				Coarse mode <sup>b</sup>			
			Mean	S.D. <sup>c</sup>	Min. <sup>d</sup>	Max. <sup>e</sup>	Mean	S.D.	Min.	Max.
Dicarboxylic acids										
Saturated normal-chain diacids										
Oxalic	C <sub>2</sub>	HOOC-COOH	135	37.4	76.0	176	40.2	14.7	22.1	60.0
Malonic	C <sub>3</sub>	HOOC-CH <sub>2</sub> -COOH	19.5	6.84	7.56	23.6	12.4	3.52	6.87	15.5
Succinic	C <sub>4</sub>	HOOC-(CH <sub>2</sub> ) <sub>2</sub> -COOH	13.4	4.98	5.08	17.5	8.02	2.21	4.66	10.1
Glutaric	C <sub>5</sub>	HOOC-(CH <sub>2</sub> ) <sub>3</sub> -COOH	3.30	1.54	1.00	4.75	1.89	0.57	1.07	2.66
Adipic	C <sub>6</sub>	HOOC-(CH <sub>2</sub> ) <sub>4</sub> -COOH	3.49	1.09	2.47	4.98	2.50	1.24	1.45	4.23
Pimelic	C <sub>7</sub>	HOOC-(CH <sub>2</sub> ) <sub>5</sub> -COOH	0.46	0.24	0.04	0.63	0.32	0.11	0.20	0.44
Suberic	C <sub>8</sub>	HOOC-(CH <sub>2</sub> ) <sub>6</sub> -COOH	0.07	0.07	0.00	0.16	0.04	0.02	0.02	0.07
Azelaic	C <sub>9</sub>	HOOC-(CH <sub>2</sub> ) <sub>7</sub> -COOH	1.20	0.72	0.51	2.41	1.15	0.60	0.49	2.10
Decanedioic	C <sub>10</sub>	HOOC-(CH <sub>2</sub> ) <sub>8</sub> -COOH	0.17	0.11	0.01	0.30	0.08	0.07	0.03	0.19
Undecanedioic	C <sub>11</sub>	HOOC-(CH <sub>2</sub> ) <sub>9</sub> -COOH	0.47	0.33	0.13	0.76	0.25	0.10	0.14	0.38
Dodecanedioic	C <sub>12</sub>	HOOC-(CH <sub>2</sub> ) <sub>10</sub> -COOH	0.07	0.03	0.03	0.09	0.05	0.02	0.02	0.07
Branched-chain diacids										
Methylmalonic	iC <sub>4</sub>	HOOC-CH(CH <sub>3</sub> )-COOH	0.43	0.23	0.09	0.71	0.47	0.37	0.09	0.99
Methylsuccinic	iC <sub>5</sub>	HOOC-CH(CH <sub>3</sub> )-COOH	0.81	0.27	0.37	1.00	0.59	0.13	0.45	0.80
2-Methylglutaric	iC <sub>6</sub>	HOOC-CH(CH <sub>3</sub> )-(CH <sub>2</sub> ) <sub>2</sub> -COOH	0.35	0.24	0.05	0.70	0.19	0.20	0.04	0.53
Unsaturated aliphatic diacids										
Maleic	M	HOOC-CH=CH-COOH - <i>cis</i>	0.81	0.25	0.41	1.05	0.73	0.23	0.37	0.95
Fumaric	F	HOOC-CH=CH-COOH - <i>trans</i>	0.31	0.09	0.20	0.42	0.21	0.08	0.12	0.30
Methylmaleic	mM	HOOC-C(CH <sub>3</sub> )=CH-COOH - <i>cis</i>	0.34	0.27	0.11	0.76	0.57	0.48	0.11	1.37
Unsaturated aromatic diacids										
Phthalic	Ph	HOOC-(C <sub>6</sub> H <sub>4</sub> )-COOH - <i>o-isomer</i>	6.29	2.85	1.99	9.3	2.79	0.81	1.85	3.9
Isophthalic	iPh	HOOC-(C <sub>6</sub> H <sub>4</sub> )-COOH - <i>m-isomer</i>	0.46	0.07	0.35	0.55	0.17	0.06	0.09	0.22
Terephthalic	tPh	HOOC-(C <sub>6</sub> H <sub>4</sub> )-COOH - <i>p-isomer</i>	2.21	1.15	0.32	3.30	0.64	0.38	0.09	1.17
Multifunctional diacids										
Malic	hC <sub>4</sub>	HOOC-CH(OH)-CH <sub>2</sub> -COOH	0.14	0.05	0.11	0.21	0.14	0.06	0.07	0.20
Ketomalonic	kC <sub>3</sub>	HOOC-C(O)-COOH	4.92	3.79	0.46	9.28	0.49	0.17	0.32	0.77
4-Ketopimelic	kC <sub>7</sub>	HOOC-CH <sub>2</sub> -CH <sub>2</sub> -HC(O)(CH <sub>3</sub> ) <sub>2</sub> -COOH	2.57	0.83	1.26	3.20	0.43	0.16	0.26	0.69
Total diacids			196	58.1	98.3	253	74.1	24.3	41.4	105
ω-Oxocarboxylic acids										
Glyoxylic	ωC <sub>2</sub>	OHC-COOH	14.1	5.92	4.77	20.2	4.81	2.00	2.23	7.20
3-Oxopropanoic	ωC <sub>3</sub>	OHC-CH <sub>2</sub> -COOH	0.08	0.05	0.00	0.12	0.05	0.04	0.02	0.12
4-Oxobutanoic	ωC <sub>4</sub>	OHC-(CH <sub>2</sub> ) <sub>2</sub> -COOH	2.23	1.12	0.86	3.56	0.68	0.35	0.41	1.22
9-Oxononanoic	ωC <sub>9</sub>	OHC-(CH <sub>2</sub> ) <sub>7</sub> -COOH	0.74	0.20	0.54	1.07	1.06	0.34	0.57	1.41
Total oxoacids			17.1	7.04	6.27	25.0	6.60	2.33	3.26	9.52
Ketoacid										
Pyruvic	Pyr	CH <sub>3</sub> -C(O)-COOH	2.61	0.76	1.67	3.48	2.32	1.20	0.76	4.09
α-Dicarbonyls										
Glyoxal	Gly	OHC-CHO	2.74	1.12	1.45	4.40	0.84	0.26	0.50	1.17
Methylglyoxal	MeGly	CH <sub>3</sub> -C(O)-CHO	1.09	0.98	0.25	2.53	0.65	0.16	0.45	0.87
Total α-dicarbonyls			2.83	1.59	1.03	4.68	1.49	0.37	0.96	1.86
Aromatic monoacid										
Benzoic acid		C <sub>6</sub> H <sub>5</sub> -COOH	16.5	11.0	4.57	28.3	1.98	1.01	0.70	3.38

<sup>a</sup>Fine mode represents aerosol size of D<sub>p</sub> < 2.1 μm.<sup>b</sup>Coarse mode represents aerosol size of D<sub>p</sub> > 2.1 μm.<sup>c</sup>Standard deviation.<sup>d</sup>Minimum.<sup>e</sup>Maximum.



**Table 3.** Pearson correlation coefficients<sup>a</sup> (*r*) matrix among the selected chemical species/components measured in the fine and coarse mode aerosols from Okinawa Island in the western North Pacific Rim.

	Fine mode <sup>b</sup>																						
	Na <sup>+</sup>	NH <sub>4</sub> <sup>+</sup>	K <sup>+</sup>	Mg <sup>2+</sup>	Ca <sup>2+</sup>	MSA <sup>-</sup>	Cl <sup>-</sup>	NO <sub>3</sub> <sup>-</sup>	SO <sub>4</sub> <sup>2-</sup>	WSOC	OC	C <sub>2</sub>	C <sub>3</sub>	C <sub>4</sub>	C <sub>5</sub>	C <sub>9</sub>	Ph	ωC <sub>2</sub>	ωC <sub>9</sub>	Gly	Benzoic	LWC	
Na <sup>+</sup>	1.00																						
NH <sub>4</sub> <sup>+</sup>	-0.25	1.00																					
K <sup>+</sup>	-0.32	0.99	1.00																				
Mg <sup>2+</sup>	0.98	-0.16	-0.23	1.00																			
Ca <sup>2+</sup>	-0.21	0.62	0.33	-0.15	1.00																		
MSA <sup>-</sup>	-0.32	0.92	0.92	-0.17	0.53	1.00																	
Cl <sup>-</sup>	0.65	-0.85	-0.85	0.58	-0.33	-0.78	1.00																
NO <sub>3</sub> <sup>-</sup>	0.65	-0.56	-0.55	0.68	0.22	0.22	-0.36	0.76	1.00														
SO <sub>4</sub> <sup>2-</sup>	-0.10	0.99	0.98	-0.02	0.59	0.89	-0.78	-0.49	1.00														
WSOC	0.10	0.91	0.93	0.16	0.30	0.79	-0.57	-0.27	0.96	1.00													
OC	0.12	0.91	0.95	0.16	0.25	0.80	-0.57	-0.32	0.93	0.99	1.00												
C <sub>2</sub>	0.12	0.89	0.85	-0.13	0.22	0.80	-0.53	-0.30	0.92	0.99	0.98	1.00											
C <sub>3</sub>	-0.05	0.90	0.89	-0.05	0.20	0.66	-0.68	-0.53	0.90	0.93	0.96	0.89	1.00										
C <sub>4</sub>	-0.12	0.96	0.95	-0.09	0.15	0.76	-0.75	-0.55	0.96	0.95	0.96	0.92	0.99	1.00									
C <sub>5</sub>	-0.12	0.99	0.96	-0.05	0.33	0.87	-0.80	-0.53	0.99	0.93	0.93	0.91	0.95	0.97	1.00								
C <sub>9</sub>	0.64	0.01	0.02	0.61	0.42	-0.16	0.46	0.47	0.10	0.20	0.39	0.38	0.33	0.23	0.09	1.00							
Ph	0.41	0.78	0.73	0.46	0.42	0.63	-0.40	-0.16	0.87	0.92	0.93	0.90	0.83	0.83	0.86	0.23	1.00						
ωC <sub>2</sub>	0.11	0.92	0.90	0.19	0.19	0.82	-0.57	-0.25	0.96	0.99	0.99	0.99	0.90	0.93	0.95	0.36	0.93	1.00					
ωC <sub>9</sub>	0.23	0.22	0.12	0.18	-0.56	-0.01	-0.32	-0.53	0.29	0.13	0.22	0.05	0.31	0.26	0.32	0.80	0.02	0.16	1.00				
Gly	0.01	0.86	0.86	0.15	0.09	0.92	-0.52	-0.07	0.86	0.89	0.82	0.93	0.70	0.78	0.85	0.21	0.85	0.92	-0.11	1.00			
Benzoic	-0.13	0.99	0.99	-0.05	-0.23	0.90	-0.27	0.46	0.99	0.96	0.99	0.93	0.91	0.96	0.99	0.12	0.85	0.96	0.21	0.90	1.00		
LWC	0.16	0.87	0.83	0.30	0.53	0.88	-0.53	-0.13	0.92	0.90	0.87	0.92	0.82	0.83	0.89	0.18	0.90	0.95	0.19	0.95	0.91	1.00	
	Coarse mode <sup>c</sup>																						
	Na <sup>+</sup>	NH <sub>4</sub> <sup>+</sup>	K <sup>+</sup>	Mg <sup>2+</sup>	Ca <sup>2+</sup>	MSA <sup>-</sup>	Cl <sup>-</sup>	NO <sub>3</sub> <sup>-</sup>	SO <sub>4</sub> <sup>2-</sup>	WSOC	OC	C <sub>2</sub>	C <sub>3</sub>	C <sub>4</sub>	C <sub>5</sub>	C <sub>9</sub>	Ph	ωC <sub>2</sub>	ωC <sub>9</sub>	Gly	Benzoic	LWC	
Na <sup>+</sup>	1.00																						
NH <sub>4</sub> <sup>+</sup>	0.60	1.00																					
K <sup>+</sup>	0.96	0.77	1.00																				
Mg <sup>2+</sup>	0.98	0.63	0.33	1.00																			
Ca <sup>2+</sup>	-0.12	0.03	-0.06	-0.29	1.00																		
MSA <sup>-</sup>	-0.15	-0.66	-0.03	-0.25	-0.02	1.00																	
Cl <sup>-</sup>	0.98	0.59	0.90	0.98	-0.27	-0.22	1.00																
NO <sub>3</sub> <sup>-</sup>	-0.30	-0.23	-0.15	-0.39	0.98	0.28	-0.55	1.00															
SO <sub>4</sub> <sup>2-</sup>	0.33	0.32	0.56	0.28	0.63	0.25	0.16	0.67	1.00														
WSOC	-0.18	-0.26	0.06	-0.20	0.23	0.55	-0.36	0.92	0.72	1.00													
OC	-0.11	-0.10	0.13	-0.10	0.21	0.36	-0.28	0.92	0.72	0.97	1.00												
C <sub>2</sub>	-0.05	0.26	0.30	0.15	0.63	0.09	-0.08	0.88	0.76	0.93	0.82	1.00											
C <sub>3</sub>	0.32	0.33	0.53	0.31	0.68	0.18	0.15	0.75	0.92	0.88	0.82	0.93	1.00										
C <sub>4</sub>	0.33	0.39	0.60	0.35	0.53	0.16	0.33	0.32	0.88	0.31	0.55	0.36	0.63	1.00									
C <sub>5</sub>	0.05	0.05	0.22	-0.06	0.62	0.32	-0.05	0.43	0.75	0.28	0.38	0.22	0.45	0.91	1.00								
C <sub>9</sub>	0.85	0.20	0.25	0.91	-0.16	-0.59	0.85	-0.31	0.18	-0.08	-0.25	0.25	0.30	0.19	-0.23	1.00							
Ph	-0.52	-0.54	-0.29	-0.54	0.73	0.59	-0.66	0.93	0.54	0.56	0.33	0.63	0.58	0.21	0.40	-0.58	1.00						
ωC <sub>2</sub>	0.23	0.37	0.85	0.68	0.12	0.42	0.59	0.23	0.73	0.53	0.52	0.53	0.76	0.60	0.32	0.23	0.21	1.00					
ωC <sub>9</sub>	0.83	0.53	0.82	0.87	-0.33	0.03	0.80	-0.22	0.21	0.07	0.16	0.28	0.38	0.08	-0.31	0.93	-0.28	0.33	1.00				
Gly	0.26	0.26	0.78	0.57	0.05	0.52	0.58	0.06	0.69	0.28	0.33	0.22	0.55	0.76	0.57	0.24	0.12	0.89	0.13	1.00			
Benzoic	-0.40	-0.60	-0.57	-0.36	-0.70	0.17	-0.29	-0.43	-0.88	-0.40	-0.35	-0.57	-0.73	-0.91	-0.77	-0.37	0.19	-0.48	-0.07	-0.51	1.00		
LWC	0.61	0.03	0.53	0.56	-0.70	0.48	0.63	-0.51	-0.10	-0.19	-0.13	-0.29	-0.08	-0.03	-0.22	0.23	-0.31	0.57	0.25	0.63	0.31	1.00	

See Table 1 and 2 for abbreviation.

<sup>a</sup>Correlation is significant at 0.05 level for the values where *r* is > 0.80.

<sup>b</sup>Fine mode represents aerosol size of D<sub>p</sub> < 2.1 μm.

<sup>c</sup>Coarse mode represents aerosol size of D<sub>p</sub> > 2.1 μm.

915 **Figure Captions**

916 **Figure 1.** A map of East Asia with the location of Okinawa Island (26.87°N and 128.25°E) and  
917 Asian countries.

918 **Figure 2.** Seven-day backward air mass trajectories (NOAA HYSPLIT) at 500 m a.g.l. (0900 UTC)  
919 for the aerosol samples (OKI-1 to OKI-5) collected in Okinawa Island. The dates given in each  
920 panel are the starting and ending times of collection of aerosol samples in Okinawa Island. Color  
921 scale shows the altitude of the air parcel.

922 **Figure 3.** Average molecular distributions of water-soluble dicarboxylic acids and related  
923 compounds in size-segregated aerosols collected in Okinawa Island.

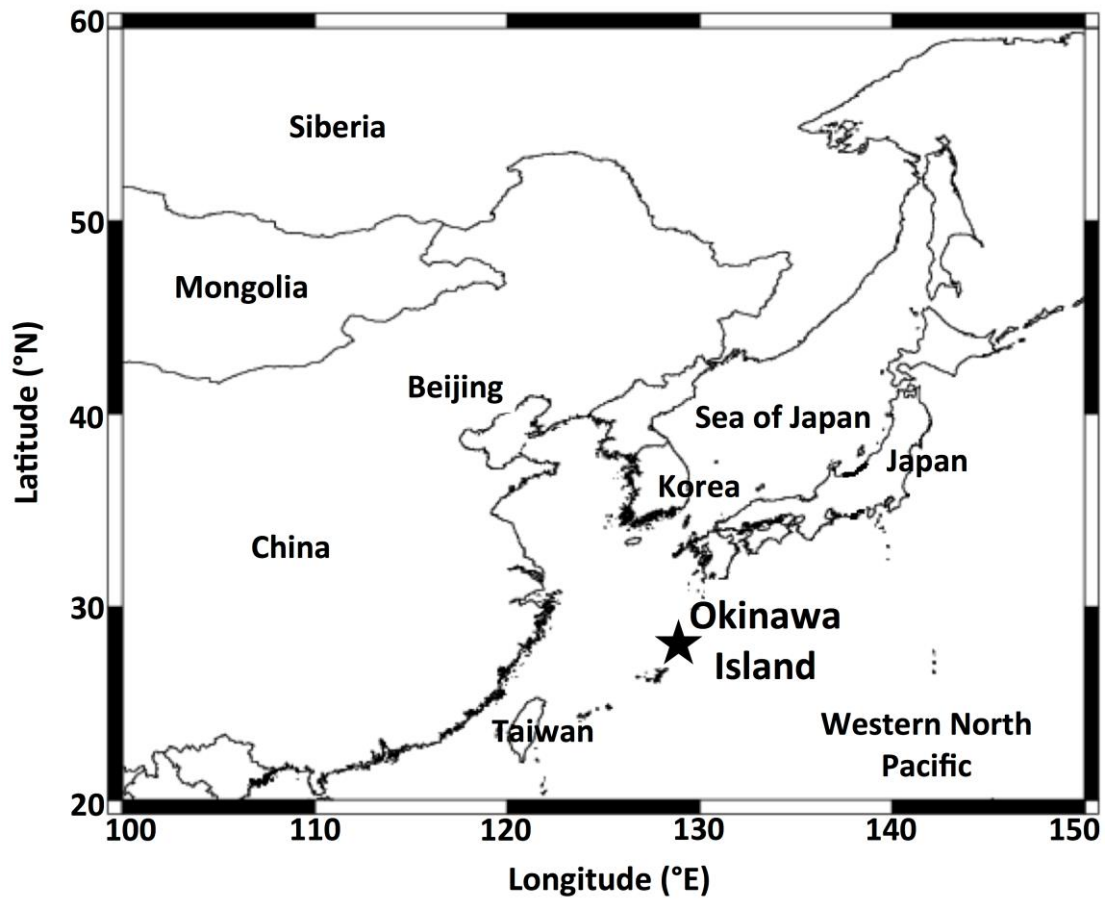
924 **Figure 4.** Size distributions of water-soluble inorganic ions in the aerosol samples collected in  
925 Okinawa Island.

926 **Figure 5.** Size distributions of selected water-soluble dicarboxylic acids and related compounds in  
927 the aerosol samples collected in Okinawa Island.

928 **Figure 6.** Size distributions of water-soluble organic carbon (WSOC) and organic carbon (OC) in  
929 the aerosol samples collected in Okinawa Island.

930 **Figure 7.** Aerosol liquid water contents for each sample in size-segregated aerosols and average  
931 liquid water contents in size-segregated aerosols in Okinawa Island.

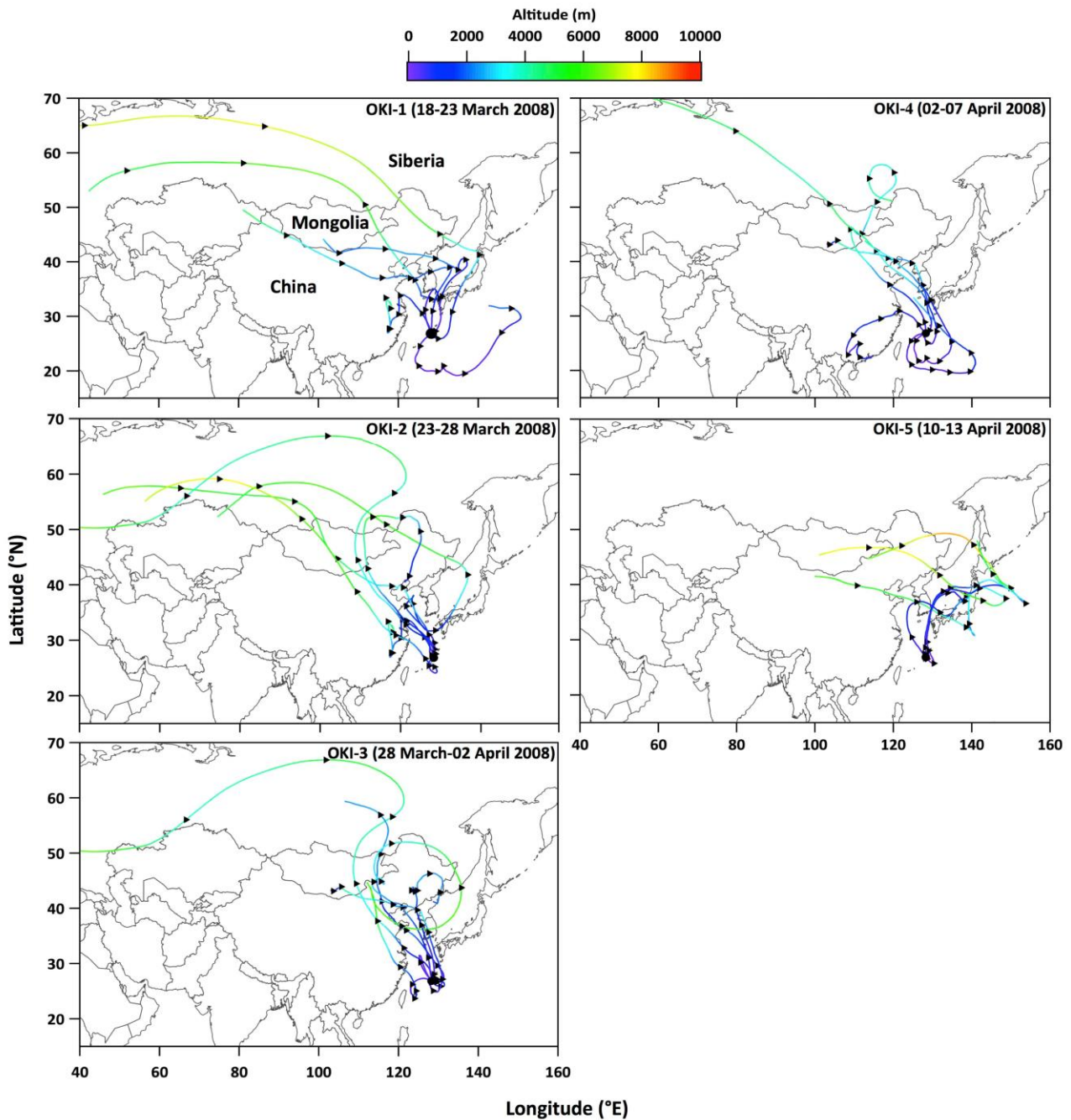
932 **Figure 8.** Mass concentration ratios of malonic to succinic acid and phthalic to azelaic acid in size-  
933 segregated aerosols collected in Okinawa Island.



934

935 **Figure 1.** A map of East Asia with the location of Okinawa Island (26.87°N and 128.25°E) and

936 Asian countries.



937

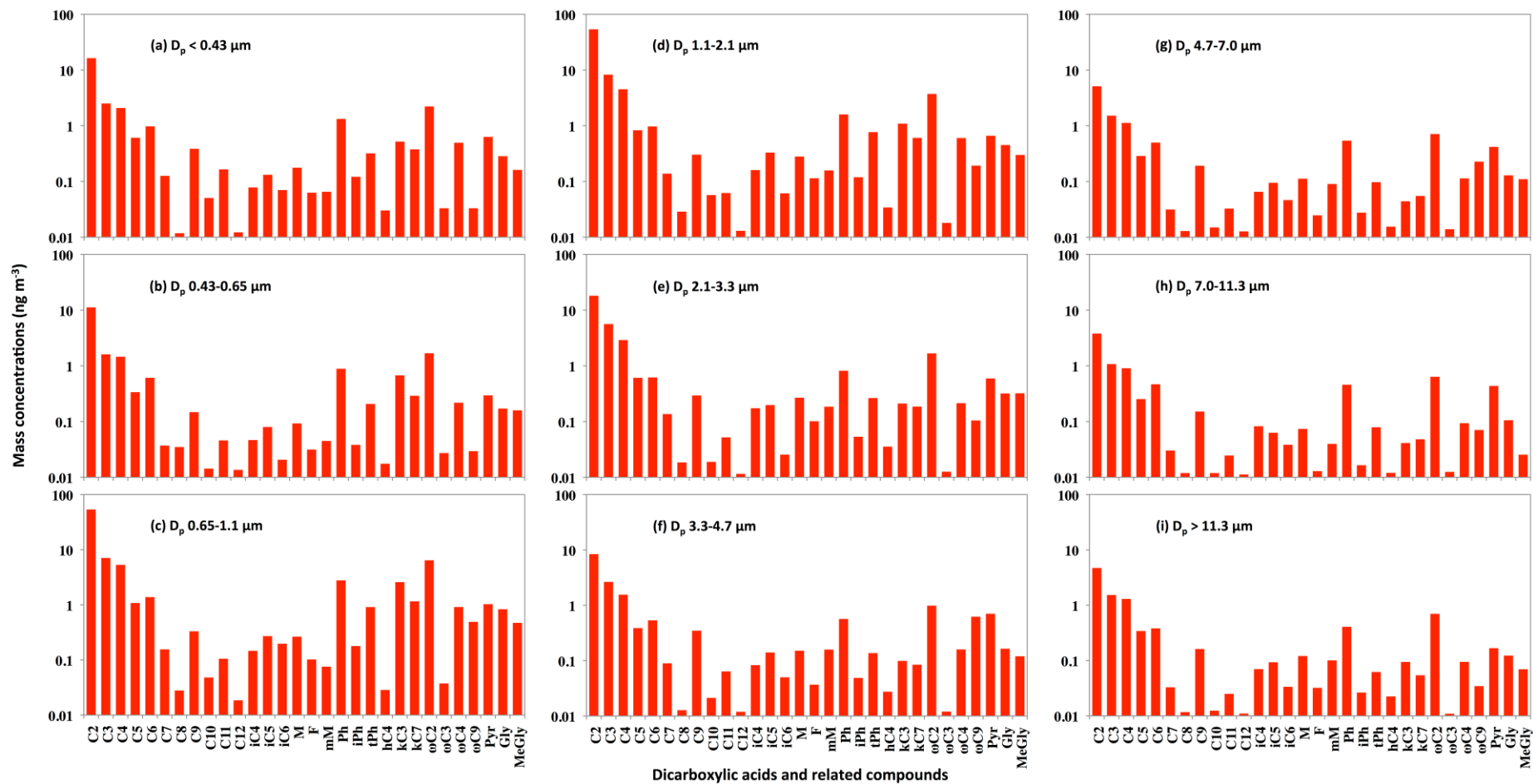
938 **Figure 2.** Seven-day backward air mass trajectories (NOAA HYSPLIT) at 500 m a.g.l. (0900 UTC)

939 for the aerosol samples (OKI-1 to OKI-5) collected in Okinawa Island. The dates given in each

940 panel are the starting and ending times of the collection of aerosol samples in Okinawa Island.

941 Color scale shows the altitude of the air parcel.

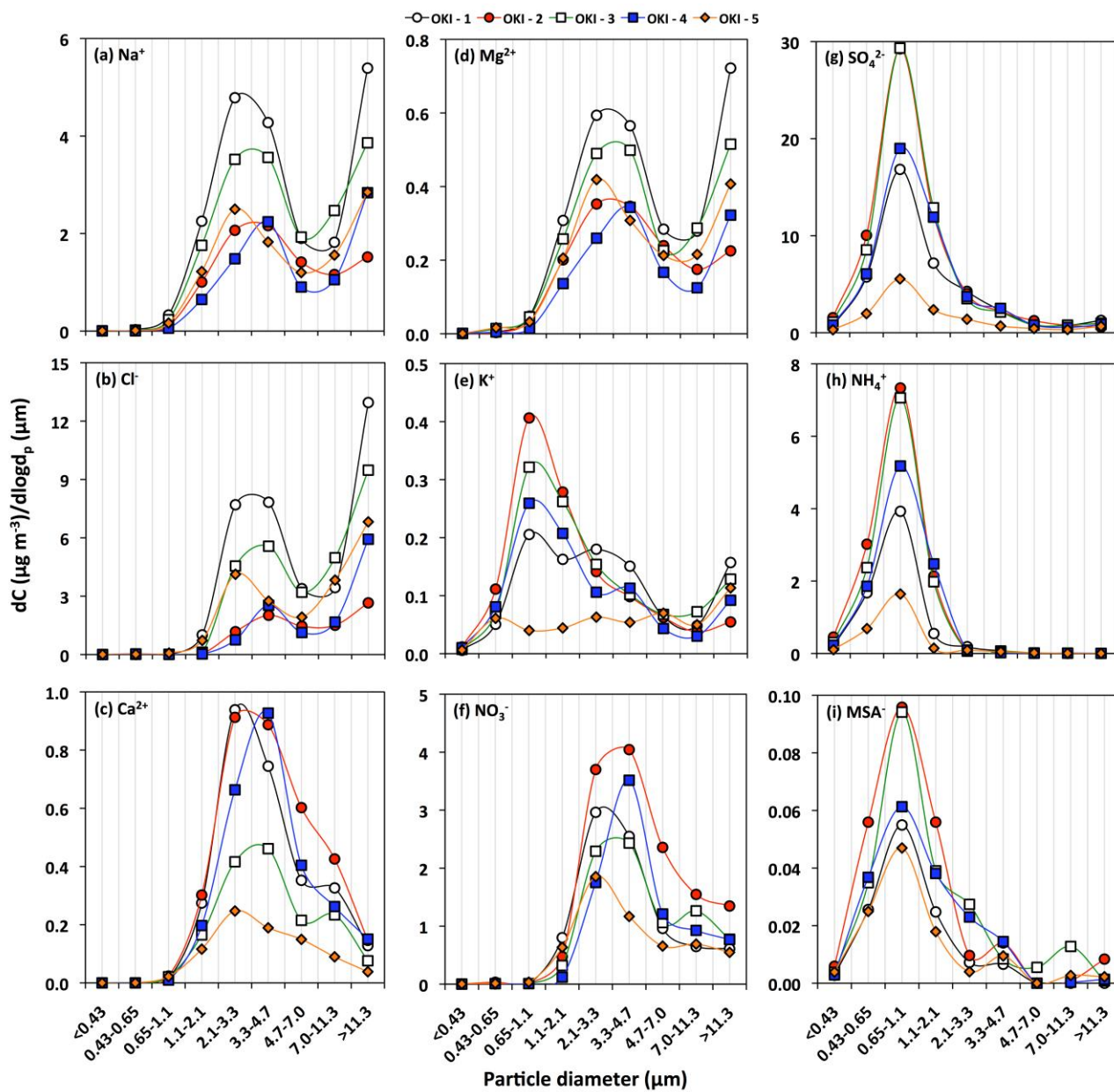
942



943

944 **Figure 3.** Average molecular distributions of water-soluble dicarboxylic acids and related compounds in size-segregated aerosols collected in Okinawa

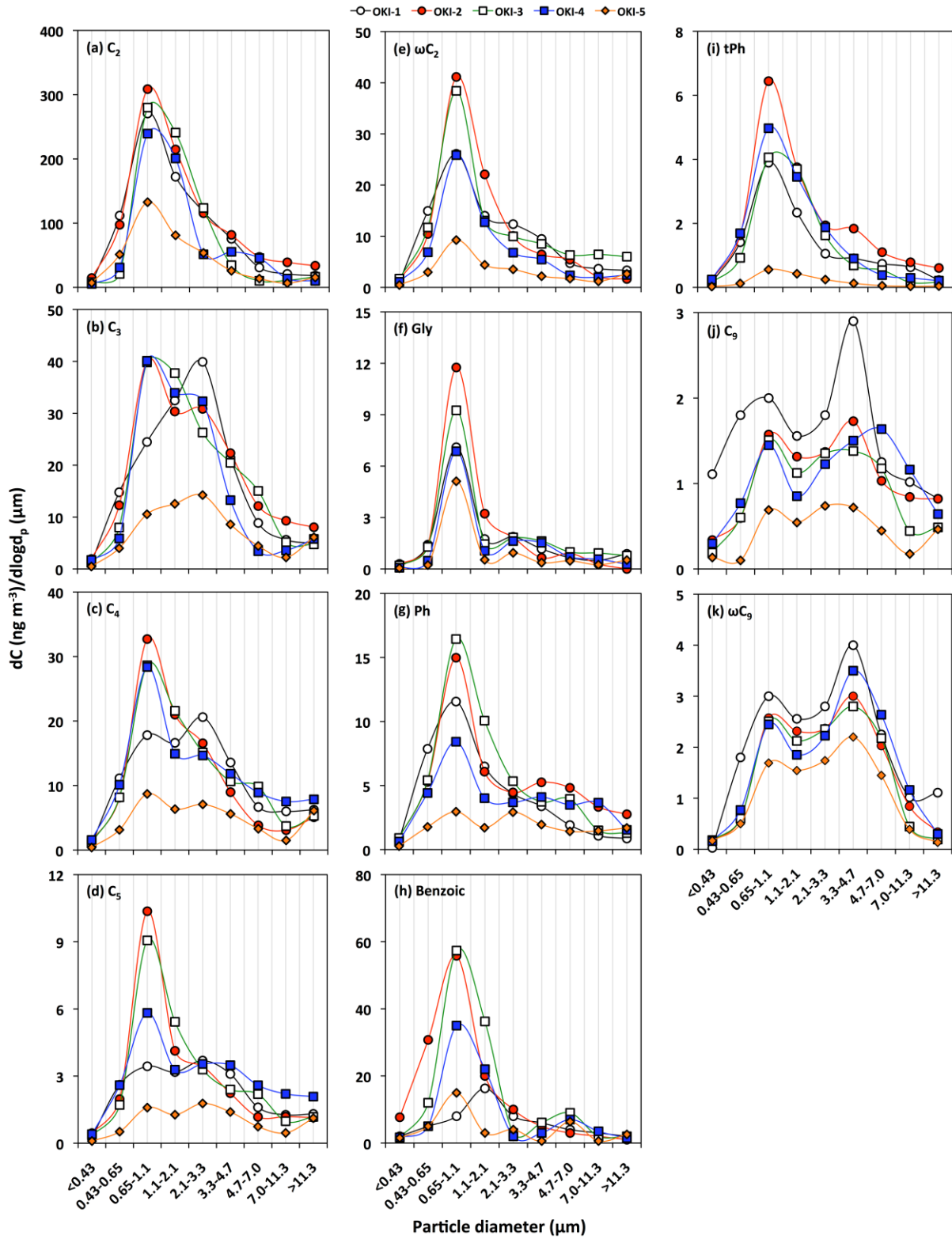
945 Island.



946

947 **Figure 4.** Size distributions of water-soluble inorganic ions in the aerosol samples collected in

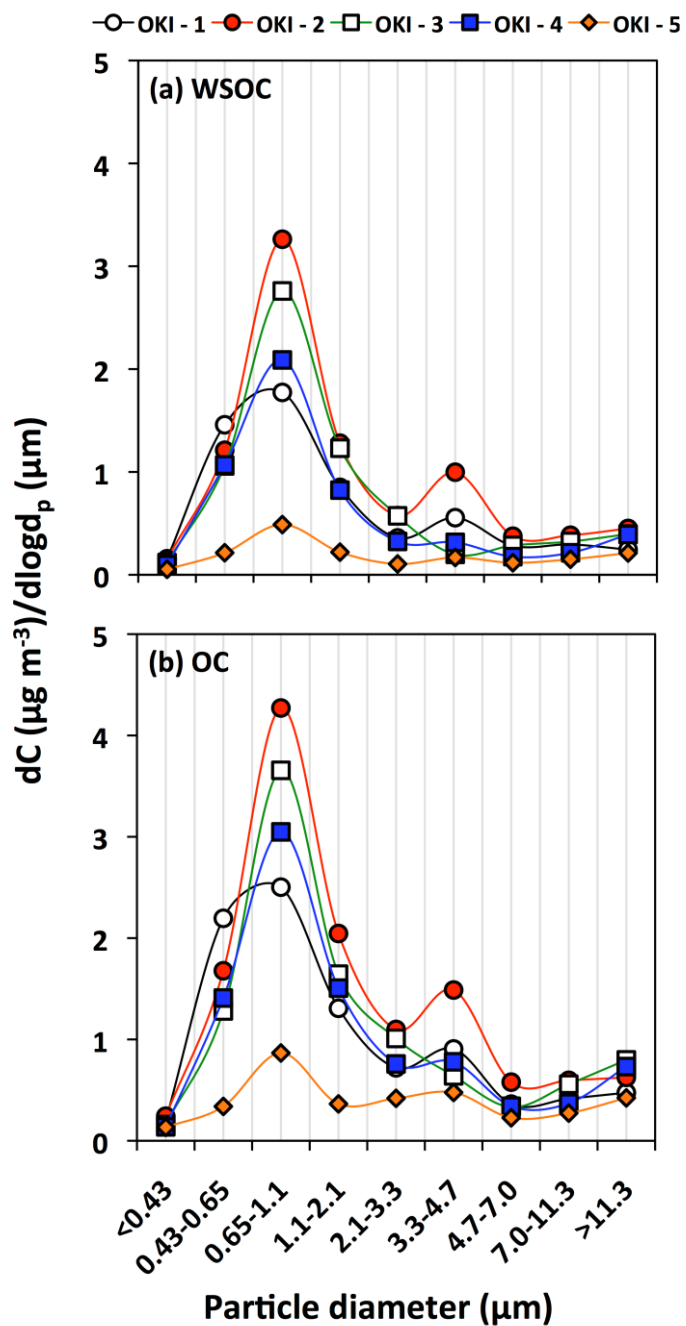
948 Okinawa Island.



949

950 **Figure 5.** Size distributions of selected water-soluble dicarboxylic acids and related compounds in  
 951 the aerosol samples collected in Okinawa Island.

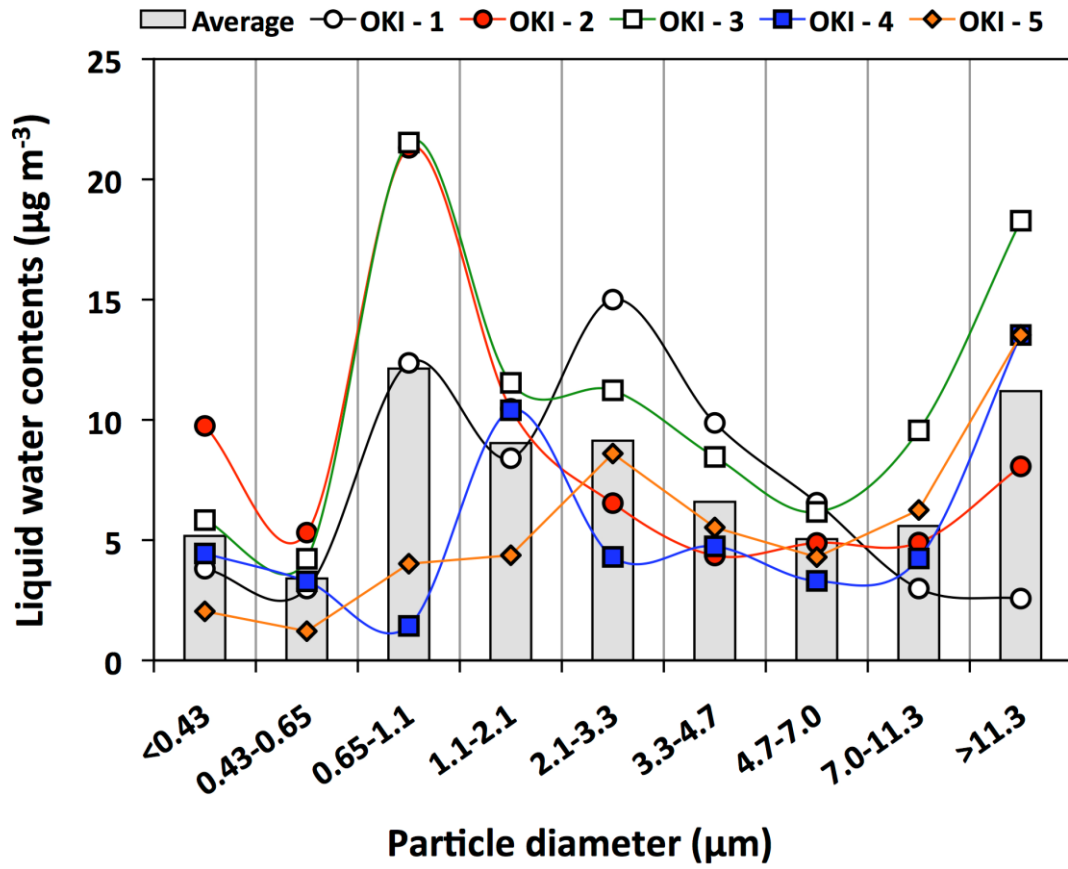
952



953

954 **Figure 6.** Size distributions of water-soluble organic carbon (WSOC) and organic carbon (OC) in  
 955 the aerosol samples collected in Okinawa Island.

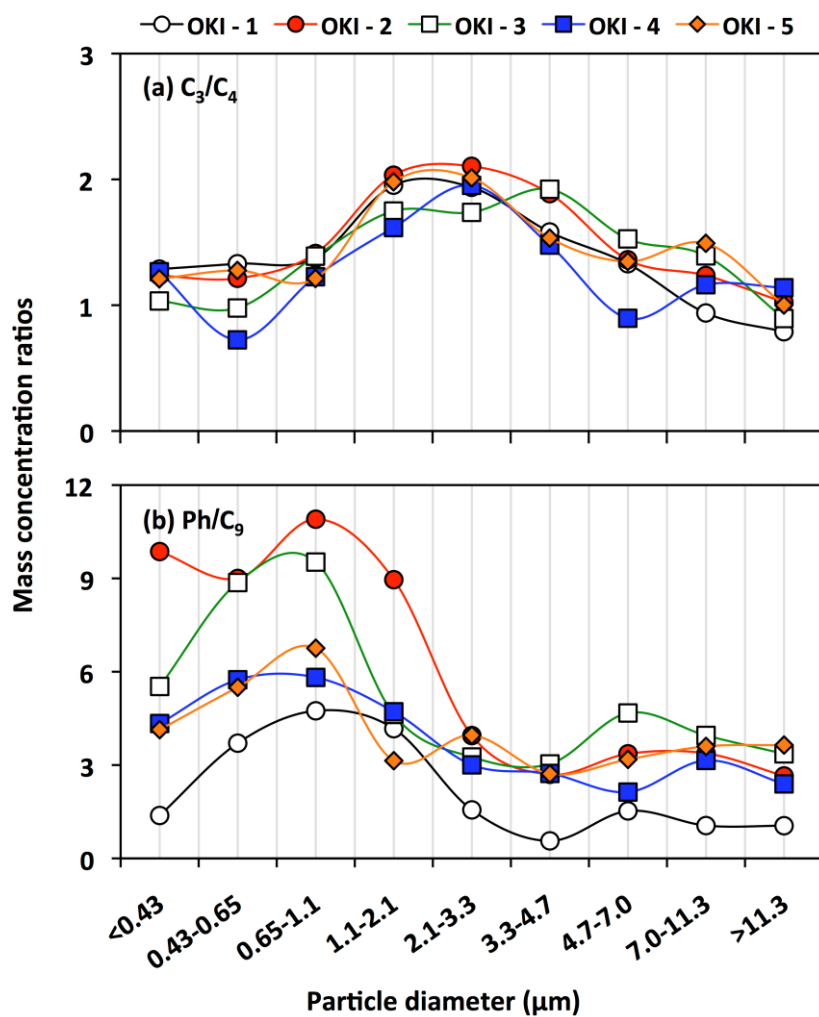




956

957 **Figure 7.** Aerosol liquid water contents for each sample in size-segregated aerosols and average  
 958 liquid water contents in size-segregated aerosols in Okinawa Island.

959



960

961 **Figure 8.** Mass concentration ratios of malonic to succinic acid and phthalic to azelaic acid in size-  
 962 segregated aerosols collected in Okinawa Island.

## Supporting Information of

**Dicarboxylic acids, oxoacids, benzoic acid,  $\alpha$ -dicarbonyls, WSOC, OC, and ions in spring aerosols from Okinawa Island in the western North Pacific Rim: Size distributions and formation processes**

**D. K. Deshmukh et al.**

**This file includes:**

**Figures:**

**Figure S1.** Seven-day backward air mass trajectories (NOAA HYSPLIT) at 500 m a.g.l. corresponding to 0900 UTC for the aerosol samples collected (OKI-1 to OKI-5) in Okinawa Island. The dates along with the sample ID are the starting and ending times for the collection of aerosol samples in Okinawa Island.

**Figure S2.** Seven-day backward air mass trajectories (NOAA HYSPLIT) at 500 m a.g.l. (0900 UTC) along with the data of (a) precipitation and (b) downward solar radiation flux for the aerosol samples collected (OKI-1 to OKI-5) in Okinawa Island. The dates given in each panel in figure are the starting and ending times of collection of aerosol samples in Okinawa Island.

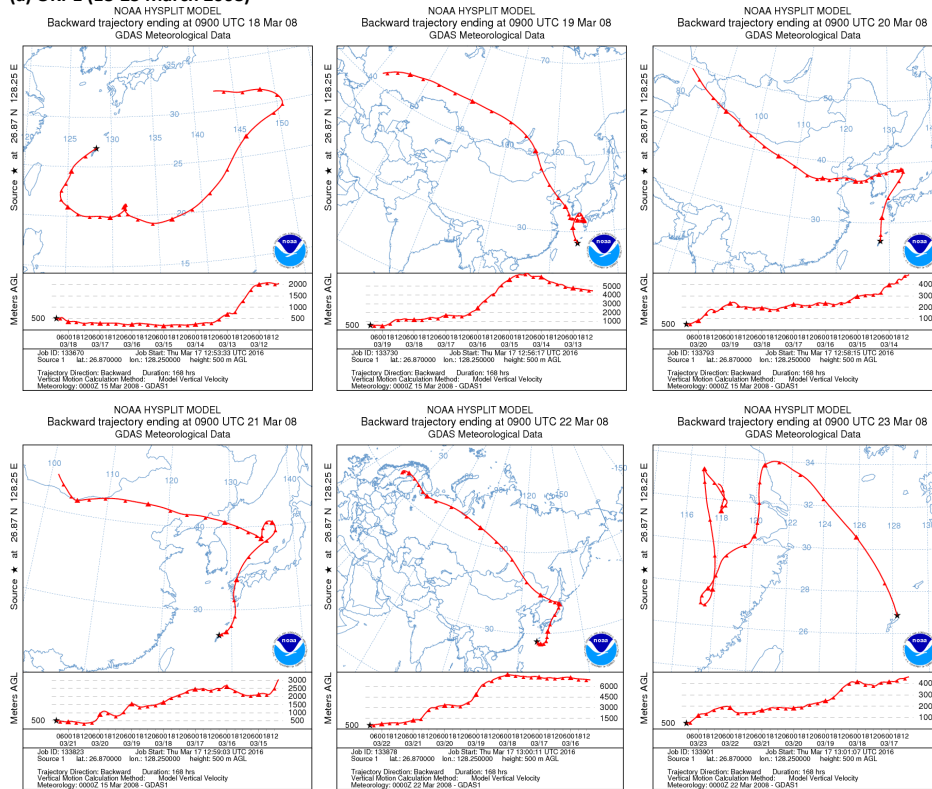
**Figure S3.** The scatter plots of  $C_2$  with  $C_3$ - $C_5$  diacids,  $\omega C_2$  and Gly in fine and coarse mode aerosols in Okinawa.

**Tables:**

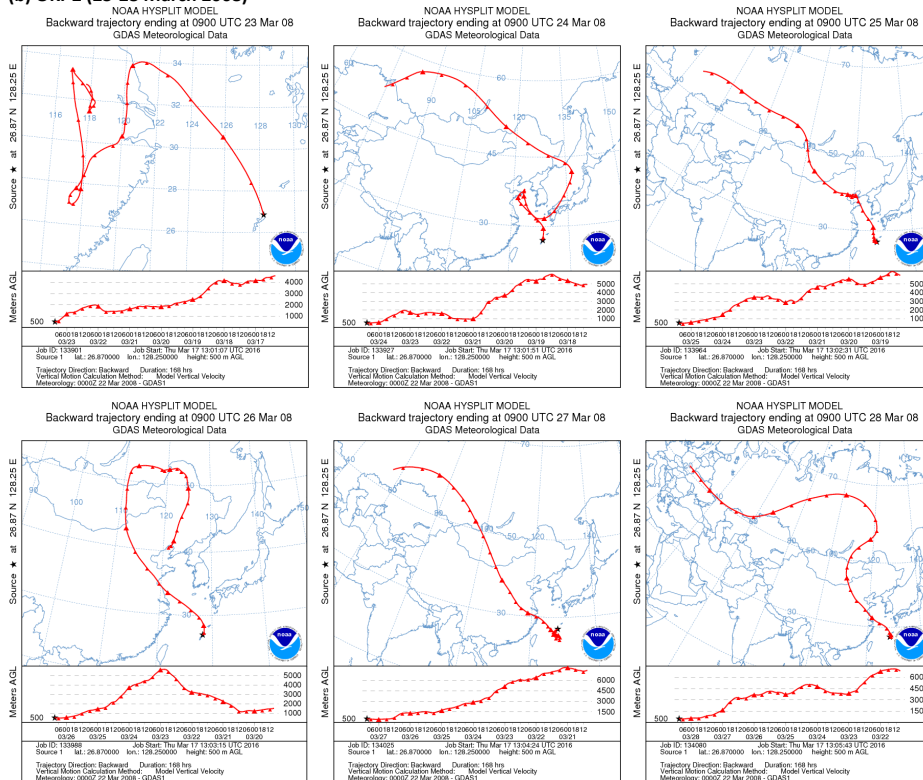
**Table S1.** Correlation coefficient ( $r$ ) and slope of the linear regression of oxalic acid ( $C_2$ ) with other diacids and related compounds together with their statistical significance between fine and coarse mode aerosols in Okinawa Island.

**Table S2.** Correlation coefficient ( $r$ ) and slope of the linear regression of oxalic acid ( $C_2$ ) with other diacids and related compounds together with their statistical significance in fine mode aerosols in Okinawa Island.

**(a) OKI-1 (18-23 March 2008)**



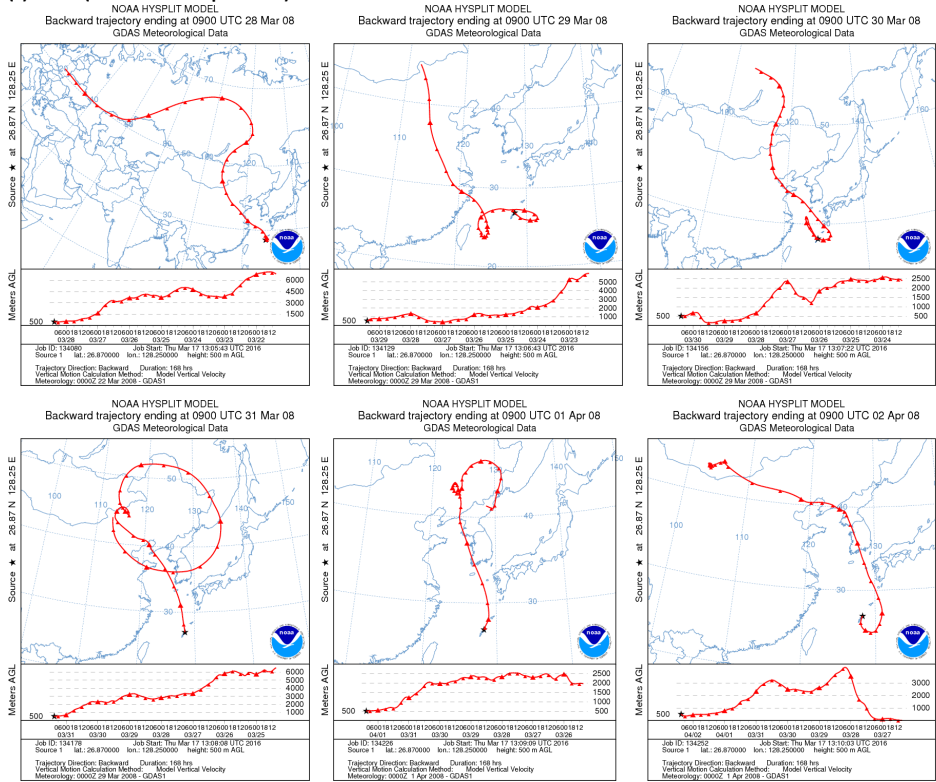
**(b) OKI-2 (23-28 March 2008)**



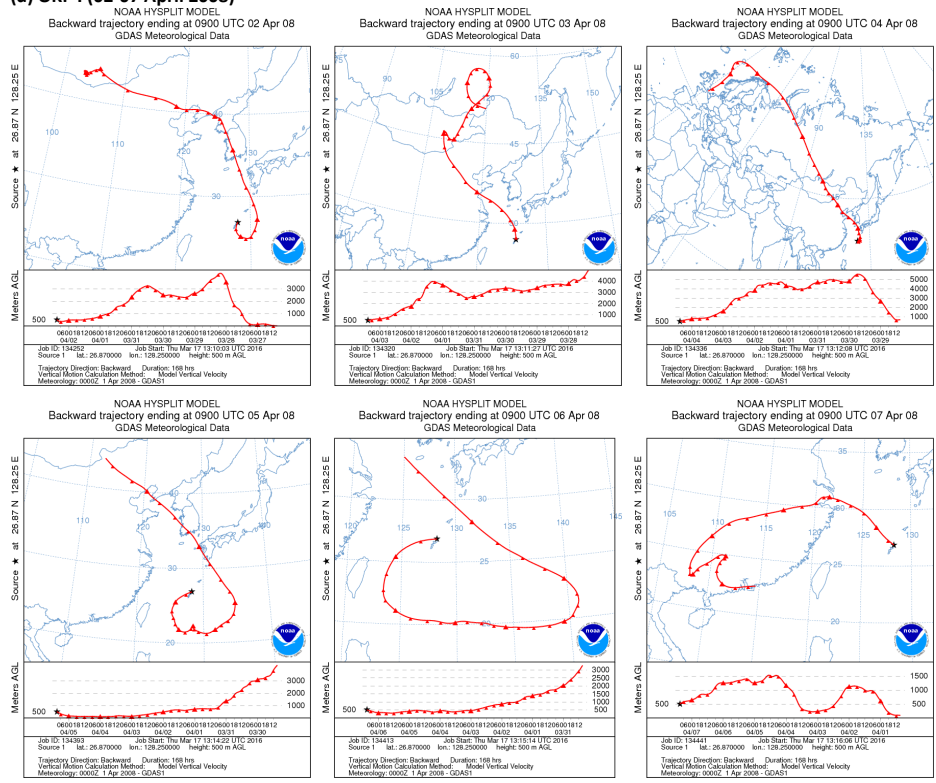
**Figure S1.** Seven-day backward air mass trajectories (NOAA HYSPLIT) at 500 m a.g.l. corresponding to 0900 UTC for the aerosol samples collected (OKI-1 to OKI-5) in Okinawa Island. The dates along with the sample ID are the starting and ending times for the collection of aerosol samples in Okinawa Island.

Figure S1 continue..

**(c) OKI-2 (28 March-02 April 2008)**



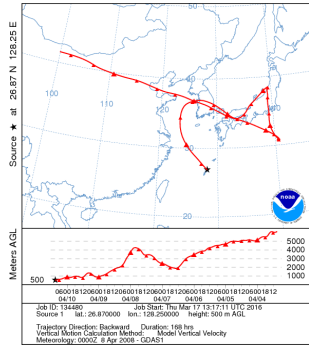
**(d) OKI-4 (02-07 April 2008)**



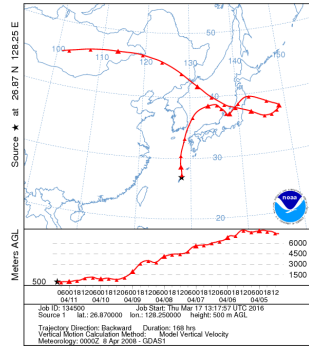
**Figure S1 continue..**

**(e) OKI-5 (10-13 April 2008)**

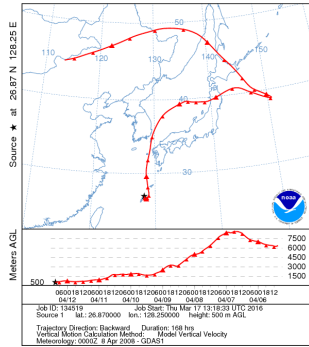
NOAA HYSPLIT MODEL  
Backward trajectory ending at 0900 UTC 10 Apr 08  
GDAS Meteorological Data



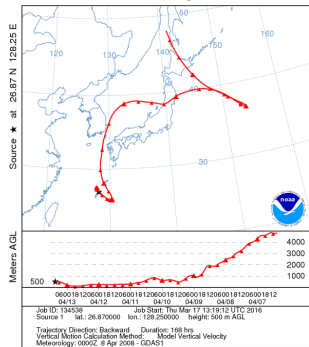
NOAA HYSPLIT MODEL  
Backward trajectory ending at 0900 UTC 11 Apr 08  
GDAS Meteorological Data



NOAA HYSPLIT MODEL  
Backward trajectory ending at 0900 UTC 12 Apr 08  
GDAS Meteorological Data



NOAA HYSPLIT MODEL  
Backward trajectory ending at 0900 UTC 13 Apr 08  
GDAS Meteorological Data



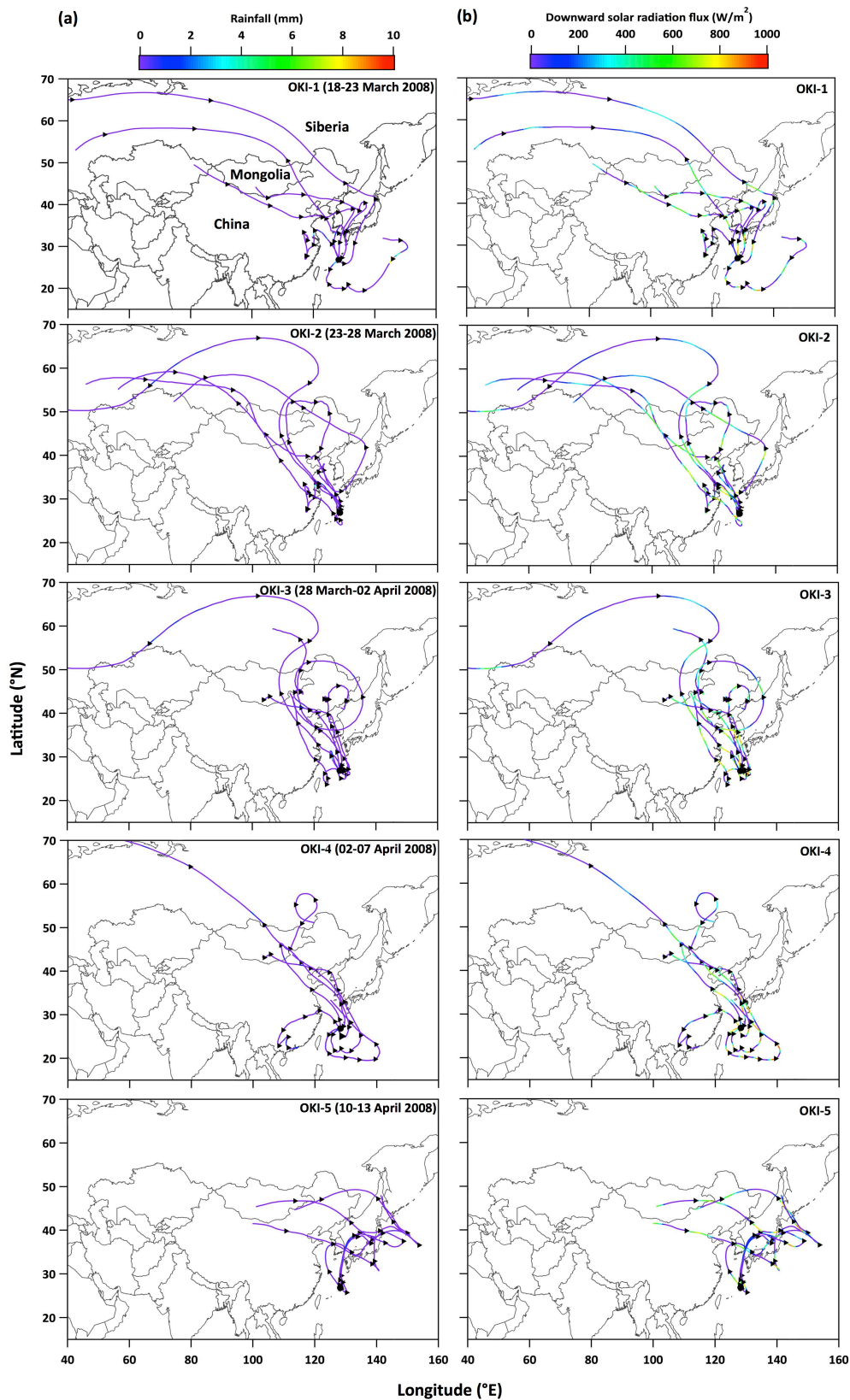


**Figure S2.** Seven-day backward air mass trajectories (NOAA HYSPLIT) at 500 m a.g.l. (0900 UTC) along with the data of (a) precipitation and (b) downward solar radiation flux for the aerosol samples collected (OKI-1 to OKI-5) in Okinawa Island. The dates given in each panel in figure are the starting and ending times of collection of aerosol samples in Okinawa Island.

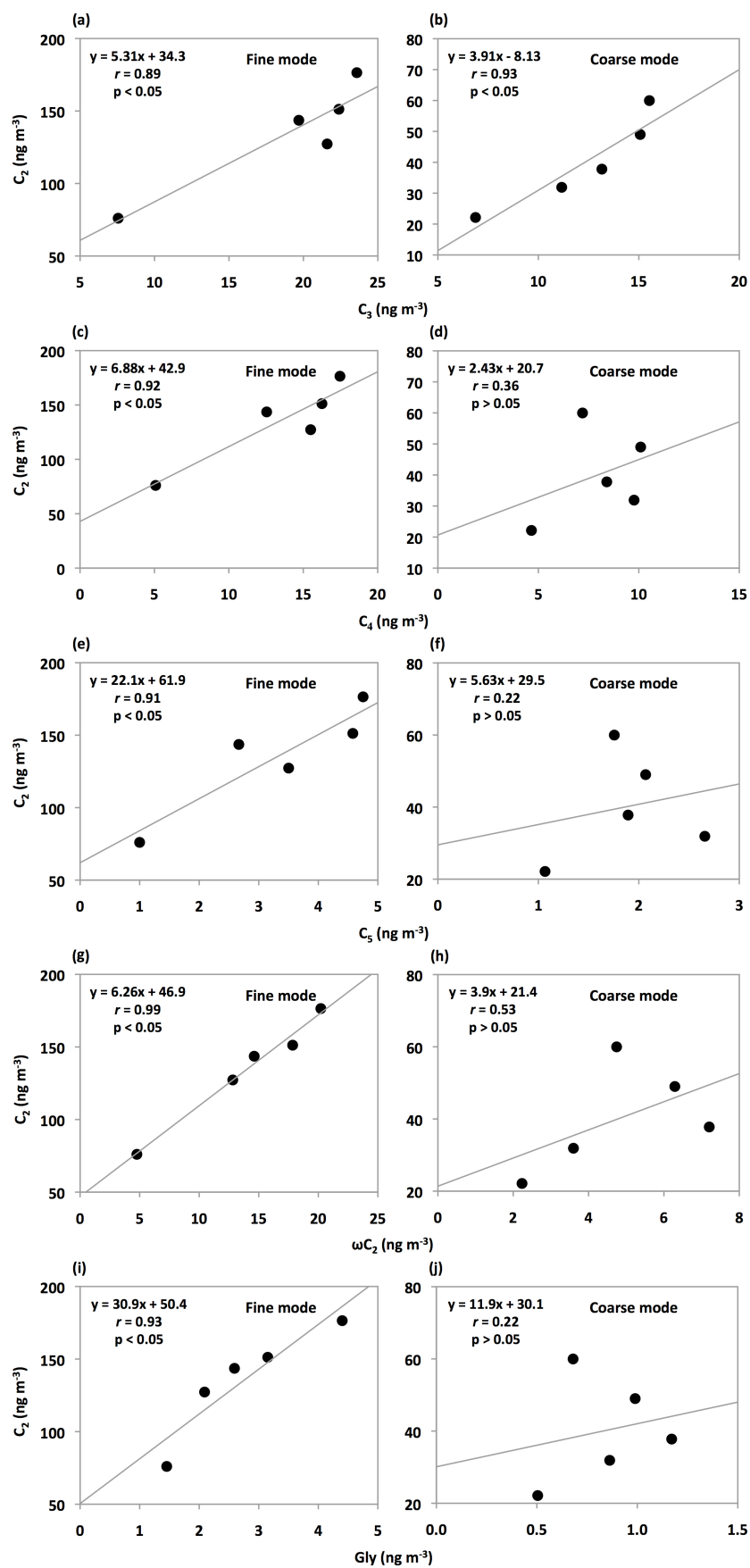


**Figure S3.** The scatter plots of  $C_2$  with  $C_3$ - $C_5$  diacids,  $\omega C_2$  and Gly in fine and coarse mode aerosols in Okinawa.



**Table S1.** Correlation coefficient ( $r$ ) and slope of the linear regression of oxalic acid ( $C_2$ ) with other diacids and related compounds together with their statistical significance between fine and coarse mode aerosols in Okinawa Island.

Linear regression	Fine mode		Coarse mode		t-score	p-value	df	t-critical at $p = 0.05$	Slope significance*
	Correlation coefficient ( $r$ )	Slope	Correlation coefficient ( $r$ )	Slope					
$C_2$ vs. $C_3$	0.89	5.31	0.93	3.91	0.92	>0.05	6	2.45	Not significant
$C_2$ vs. $C_4$	0.92	6.88	0.36	2.43	1.12	>0.05	6	2.45	Not significant
$C_2$ vs. $C_5$	0.91	22.1	0.22	5.63	2.61	<0.05	6	2.45	Significant
$C_2$ vs. $\omega C_2$	0.99	6.26	0.53	3.90	0.65	>0.05	6	2.45	Not significant
$C_2$ vs. Gly	0.93	30.9	0.22	11.9	2.53	<0.05	6	2.45	Significant

See Table 2 for abbreviation.

df = degree of freedom.

\*If, t-score > t-critical => reject null hypothesis => difference in the slope is significant.

**Table S2.** Correlation coefficient ( $r$ ) and slope of the linear regression of oxalic acid ( $C_2$ ) with other diacids and related compounds together with their statistical significance in fine mode aerosols in Okinawa Island.

Linear regression	Correlation coefficient ( $r$ )	Slope	Linear regression	Correlation coefficient ( $r$ )	Slope	t-score	p-value	df	t-critical at $p = 0.05$	Slope significance*
$C_2$ vs. $C_3$	0.89	5.31	$C_2$ vs. $C_4$	0.92	6.88	0.73	>0.05	6	2.45	Not significant
$C_2$ vs. $C_3$	0.89	5.31	$C_2$ vs. $C_5$	0.91	22.1	2.83	<0.05	6	2.45	Significant
$C_2$ vs. $C_4$	0.92	6.88	$C_2$ vs. $C_5$	0.91	22.1	2.51	<0.05	6	2.45	Significant
$C_2$ vs. $\omega C_2$	0.99	6.26	$C_2$ vs. Gly	0.93	30.9	3.36	<0.05	6	2.45	Significant

See Table 2 for abbreviation.

df = degree of freedom.

\*If, t-score > t-critical => reject null hypothesis => difference in the slope is significant.